We are IntechOpen, the world's leading publisher of Open Access books Built by scientists, for scientists

6,900
Open access books available

185,000
International authors and editors

200M
Downloads

Our authors are among the

154
Countries delivered to

TOP 1%
most cited scientists

12.2%
Contributors from top 500 universities



WEB OF SCIENCE™

Selection of our books indexed in the Book Citation Index in Web of Science™ Core Collection (BKCI)

Interested in publishing with us?
Contact book.department@intechopen.com

Numbers displayed above are based on latest data collected.
For more information visit www.intechopen.com



Chapter 15

The Significance of Equi-Biaxial Bubble Inflation in Determining Elastomeric Fatigue Properties

Steve Jerrams, Niall Murphy and John Hanley

Additional information is available at the end of the chapter

http://dx.doi.org/10.5772/50099

1. Introduction

"I disapprove of certainties, said Virgil Jones. They limit one's range of vision. Doubt is one aspect of width."[1]

As yet, there are few certainties in the determination of fatigue life for rubber components. Scepticism is an essential characteristic for a researcher and the study of elastomeric fatigue is a prodigiously wide topic. Rubber components predominantly fail in fatigue and so determining elastomeric component fatigue life has acquired greater interest for materials scientists in recent years. Fatigue testing to date has generated results with specimens loaded in uniaxial tension, combined tension and torsion or in shear. While these test methods provide much useful insight into the fatigue of elastomers, they do not describe the full spectrum of elastomeric material behaviour under cyclic loading. In this light, dynamic bubble inflation offers a reliable and repeatable method for determining viscoelastic characteristics of rubber-like materials. The development of an equi-biaxial bubble inflation system is a central feature of this chapter, which also highlights the research projects that made the system development possible.

Perhaps the most comprehensive overview of elastomeric fatigue was provided by Mars and Fatemi in 2004 [1], though inevitably there has been extensive research into the topic since then. At the time, they placed factors influencing elastomer fatigue into four categories: mechanical loading history, environmental effects, rubber formulation and effects due to dissipative aspects of the constitutive response of rubber. They pointed out that fatigue failure of rubber-like materials was imperfectly understood and, despite gaining significant new knowledge in the intervening years, this remains the case. Factors influencing crack nucleation and growth were the subject of numerous previous

[1]A quote from the novel Grimus (ISBN: 0575018712) by Salman Rushdie, published by Gollancz (1975)

INTECH
open science | open minds

© 2012 Jerrams et al., licensee InTech. This is an open access chapter distributed under the terms of the Creative Commons Attribution License (http://creativecommons.org/licenses/by/3.0), which permits unrestricted use, distribution, and reproduction in any medium, provided the original work is properly cited.

investigations [2, 3, 4]. Mechanical loading history is important in the fatigue analysis of all engineering materials and so frequencies, stress and strain ranges, strain energy and energy release rates are obvious parameters to be considered. However, the interpretation of complex loading histories is problematical and a practical approach to avoiding this difficulty is offered in this text. A further consideration for rubber is that whereas a high steady load at sub-fracture level will not induce failure in a conventional linear solid, this is not always so for elastomers, where time dependent crack growth and environmental attack can ultimately cause a component to fail. Though such failures cannot be attributed to fatigue, since no cyclic deformation takes place, non-strain crystallizing elastomers can still fail over time. However, additional consideration must be made of the role played by strain crystallization in limiting crack growth in some elastomers, notably natural rubber (NR) and also whether cyclic load applications open or close internal flaws. Many procedures for physical testing of rubber had their roots in methods that were applied to testing metals. These procedures are often far less effective for elastomers. Consider the tendency to cycle samples through constant strain limits [5, 6] which makes perfect sense for the micro-strains experienced by steel or aluminium alloy, but a rubber sample subject to set and stress relaxation will be cycled through an ever decreasing load range, so a fatigue test can be inordinately long or the component may not fail at all. Conversely, if a rubber sample is cycled between constant load limits, there is always the possibility that the strain will increase to a level where the stroke of the test machine is exceeded. Clearly, the choice of test methods and parameters in fatigue testing of rubber is far from simple. Decisions to plot fatigue data against parameters used for metals (minimum stress, maximum stress, maximum strain, stress amplitude) are arbitrary and again an alternative approach is suggested in this text. Mars and Fatemi [7] highlighted a lack of understanding of the effects of multi-axial fatigue loading of elastomers and pointed to a tendency to use thin laboratory specimens though, unlike linear elastic solids, rubbers experience significant size effects [8, 9]. They concluded that the following factors are important;

- the relationship between the applied loads and the localised load experienced by a crack,
- whether or not applied loads cause closure of initial cracks
- the dependence of material properties on the type and magnitude of the imposed deformation (e.g. the role that might be played by strain crystallisation).

Loading frequency has little effect on the fatigue properties of strain crystallising rubbers, but has a significant effect on amorphous rubbers that has been attributed to time-dependent steady crack growth [10]. At high frequencies and strains, rubber experiences a further failure mechanism termed thermal runaway, where compound temperatures increase rapidly and degradation ensues [11]. The fatigue properties of amorphous rubbers are considered to be more influenced by waveform than those of strain crystallising elastomers, but this is highly dependent on polymer and filler types [12].

Environmental conditions are particularly important in affecting fatigue processes for elastomers. Fatigue life can fall and crack growth rate increase markedly as a result of

temperature increase and these outcomes are independent of chemical changes due to aging or continued vulcanisation, though temperature increases clearly accelerate chemical processes. Exposure to Ozone increases crack growth rate and reduces fatigue life [13]. In the vicinity of stress concentrations occurring at the crack tip, network chains react with ozone, causing scissions of the chains, though other chemical agents can attack rubber in the same way [14]. Oxidative aging of rubber causes the material to become more brittle and accelerates fatigue crack growth [15].

Rubber fatigue behaviour is influenced by polymer type, filler type and volume fraction. Additionally, the manufacturing process and the amount and type of antioxidants, antiozonants and curatives will have an effect. Again, whether or not the compound exhibits strain crystallisation is a key factor; strain crystallising rubbers are less prone to environmental effects [16]. Carbon black improves fatigue properties with low-structure blacks imparting superior properties to high-structure blacks [17].

In the past few years, the increased use of finite element techniques to facilitate elastomeric fatigue life prediction has become more prevalent [18], along with novel approaches to predict discontinuous crack growth [19]. Similarly, greater use of tomography has occurred, particularly in the study of heat build up during cycling [20, 21, 22] and X-ray diffraction plays an important part in investigations of fatigue mechanisms [23]. Scanning Electron Microscopy (SEM) and Digital Image Correlation (DIC) techniques have each been used more extensively to study crack morphology and growth in the last decade [24, 25]. The research of Le Cam and Toussaint is particularly illuminating in respect of crack bifurcation under non-relaxing conditions [26] and cavitation [27] and McNamara *et al* have developed Image Correlation Photogrammetry (ICP) to study stress softening in successive cycles at stress-raisers in a range of compounds [28].

Improvements in engineering materials are continually sought as functionality, reliability and resilience are demanded from the machines that we depend upon each day. As our understanding of elastomeric material behaviour has advanced, there has been an accompanying realisation that obtaining reliable multi-axial dynamic data is essential in fully characterising the hyperelastic and viscoelastic properties of rubber. When machine components fail, they should and usually do fail in fatigue. For them to fail under static loading would indicate that designs or material selections were inept. As there is an increasing threat to natural resources, ensuring that components exhibit longevity has gained heightened importance. Hence, understanding fatigue and designing to obviate premature failures is essential. This text describes interrelated fatigue research programmes spanning a fifteen year period from the inception of a static bubble inflation system, a novel approach to elastomer fatigue life prediction using Wöhler (S/N) curves, the consideration of pre-stressing and dynamic stored energy, an appraisal of the contribution made by flaw size in inducing fatigue failure in rubber samples, cyclic bubble inflation to provide reliable fatigue data and culminates in a study of swelling phenomenon in diaphragms.

2. Approaches to determining the fatigue life of elastomers

Fatigue life prediction for rubber components can be approached in two ways:

a. By using fracture mechanics methods as epitomised by the research of Busfield *et al* [29] and Thomas [30].
b. By relating the magnitude of a parameter during cycling (e.g. stress amplitude, maximum stress, maximum strain or stored energy) to the cycles to failure. These relationships are shown in Wöhler (S/N) curves derived from cycling standard test-pieces to failure (Abraham *et al* [31]).

In the first approach, Mechanical fatigue of elastomers is characterised by a reduction of physical properties as a result of crack propagation during dynamic excitation. There are levels of stress and strain below which fatigue damage will not occur, but these levels are imperfectly understood. Energy concepts of elastomeric fatigue life determination are based on energy release rates and have their origins in the theories first postulated by Griffith [32]. It is assumed that the energy of a cracked sample will be entirely converted into crack surface energy during repeated loading. However, when characterising crack propagation in rubber, two unique problems must be surmounted:

i. Fatigue properties are not merely dependent on chemical composition, but also on individual considerations such as cross linking systems and aging protection used in the compound.
ii. The combination of hyperelastic and viscoelastic properties gives rise to sensitivity to loading modes and frequencies, strain rates and temperatures.

2.1. Fracture mechanics approach

Rivlin and Thomas [33] first offered approaches to determining energies in crack growth of rubber specimens, defining tearing energy T as the decrease in elastic strain energy caused by the crack growth per unit area, giving rise to the relationship shown in Equation 1.

$$T = \left(\frac{\delta W}{\delta A} \right)_l \tag{1}$$

where W is the total elastic energy, A the crack area and l denotes that the specimen is held under constant deformation, so the application of applied external forces does no additional work.

Under tensile loading of a notched specimen, tearing energy can be expressed as

$$T = 2kW_0c \tag{2}$$

where W_0 is the strain energy per unit volume, c is the crack length and k a constant given by

$$k = \frac{\pi}{\lambda} \qquad [34, 35, 36](3)$$

Tearing energy of a notched sample under tensile loading can be calculated using Equation (2) by replacing W_0 with strain energy density W_{max} at stretch ratios of $\lambda = \lambda_{max}$. The fracture mechanics approach can be used to relate initial flaw size to fatigue life. At intermediate and high tearing energies, fatigue behaviour can be approximately described by Equation (4)

$$\frac{dc}{dN} = BT^{\beta} \tag{4}$$

where B and β are material constants

By integrating Equation (4) and substituting Equation (2) for T, an expression for cycles to failure N is derived (Equation (5)).

$$N = \frac{1}{\beta - 1}\left[\frac{1}{\beta\left(2kW_0\right)^{\beta}}\right]\left[\frac{1}{c_0^{\beta-1}} - \frac{1}{c^{\beta-1}}\right] \tag{5}$$

Using this expression can be problematical since material constants from short-term testing are used to extrapolate fatigue lives for un-notched specimens.

2.2. Wöhler (S/N) curves

As early as 1870, Wöhler [37] summarised his studies on fatigue in steam train axles, pointing to the importance of stress amplitude and the existence of a 'fatigue limit' for steel components. Thereafter, Wöhler (or S/N) curves became a standard method for determining fatigue life in linear elastic solids. Most commonly, alternating stress σ_a or $\log_{10} \sigma_a$ (ordinate), is plotted against cycles to failure N (abscissa) and usually the latter scale is logged ($\log_{10}$). The magnitude of mean stress σ_m, where components are pre-stressed ($\sigma_{min} \neq 0$), is a critical factor in fatigue life prediction and several approaches (e.g. Haigh and Goodman diagrams) have been used to determine its influence.

3. Uniaxial fatigue testing of elastomers

It is well documented that for strain crystallising rubber, crack growth steps during repeated loading are small if the material is not fully relaxed between each cycle [38]. A crystalline region develops at the crack tip and the crystallinity remains for repeated load cycles. Consequently crack growth is inhibited and fatigue life is prolonged. Increased fatigue (or crack growth) resistance with increased minimum strain is accompanied by an increase in hysteresis. Lake [39] showed that higher hysteresis caused lower crack growth and subsequently Lindley [40] showed that the high strain hysteresis was due to strain induced crystallisation. However, improved fatigue resistance in non-strain crystallising rubbers subjected to preloading had not been observed. When compared with strain

crystallising elastomers, Gent [38] and others [41, 42] found no comparable improvement in fatigue properties for filled non-crystallising elastomers subjected to a pre-stress prior to cycling between tensile stress limits. These results were confirmed by Lindley [10]. By contrast with strain crystallising rubbers like NR, the hysteresis of non-strain crystallising rubbers results from viscoelastic behaviour and is generally of a lower order.

Possible reasons for increased fatigue life for higher mean stresses (where a pre-load is applied prior to cycling at a constant stress or strain amplitude) have been advanced and are discussed in points a) - d).

a. Compressive and tensile loading of elastomers each reduce the effective severity of natural flaws. Natural flaws are unavoidable and for many years were thought to have an effective initial size of 25 μm and were considered equivalent to a sharp edge cut of approximately 40 ± 20 μm in depth [43]. If a compressive pre-load closes a stress raiser and a tensile pre-load 'smoothes out' a stress concentration [44], it is arguable that stress cycles become less injurious throughout a fatigue test.

b. Discounting the effect of hysteresis, the strain energy or tearing energy available in each cycle to propagate a crack can be less when σ_{min} or ε_{min} is not zero. This situation is shown diagrammatically in Figure 1 where equal load amplitudes do not equate to equal values of 'dynamic stored energy'. This explanation is consistent with the tearing (energy) approaches described earlier and is considered further in the next section.
c. Lee and Donovan [45] established that carbon black increases the size of the crystallised zone at a stressed crack tip.
d. Lake *et al* [46] have shown that certain non-crystallising rubbers experienced the formation of anisotropic structures resulting from filler particle alignment or aggregates at the crack tips. In tests on samples that were not completely relaxed between cycles, this produced similar increases in fatigue strength to those observed in tests on strain crystallising rubbers.

3.1. Uniaxial fatigue testing of non-strain crystallising elastomers

Abraham [47] investigated the fatigue life and dynamic crack propagation behaviour of non-strain crystallising elastomers to determine their dependency on test parameters. The research culminated in recommendations of criteria for precise prediction of service life for components formed from these compounds. Fatigue life was investigated for EPDM and styrene-butadiene rubber (SBR) dumbbell specimens. The chemical compositions of the materials are given in Tables 1 and 2 respectively.

The specimens were cycled to failure under load control at 1 Hz. The frequency was chosen to avoid internal friction causing large increases in temperature and consequent thermal breakdown [48]. For this reason, the 1 Hz frequency was subsequently adopted by Jerrams *et al* [49] for all equi-biaxial cyclic testing. The influence on fatigue properties of varying minimum stress for a constant stress amplitude was investigated and confirmed the well-known amplitude dependence of fatigue life in filled rubbers. Raising the level of minimum

stress (and consequently mean and maximum stress for a constant stress amplitude), applied to uniaxial test samples, was found to produce an increase in fatigue life. This cannot be attributed to strain crystallisation as is the case for NR. It appeared that this effect was specific to filled systems and the research showed that the fatigue behaviour of carbon black filled non-strain crystallising rubbers cannot be universally described using a maximum stress or a maximum strain criterion. As a result, an energy criterion was postulated.

EPDM	100.0 pphr
Carbon black N550	70.0 pphr
Carbon black N772	40.0 pphr
Stearin acid	1.0 pphr
Zinc-oxide	5.0 pphr
Oil Sunpar 2280	70.0 pphr
Sulphur	1.5 pphr
Vulcanising agent CZ (CBS)	1.0 pphr
Vulcanising agent Thiuram (TMTD)	0.8 pphr

Table 1. Chemical composition of the filled EPDM material.

SBR 1712	100.0 pphr
Carbon black N234	51.0 pphr
Stearin acid	1.45 pphr
Zinc-oxide	2.2 pphr
GPPD	1.45 pphr
TMQ	0.73 pphr
Antilux 500L	1.45 pphr
Sulphur	1.27 pphr
Vulcanising agent CZ (CBS)	0.73 pphr
DPG	0.29 pphr

pphr = parts per hundred rubber

Table 2. Chemical composition of the carbon black filled SBR material

Another important effect was highlighted in this research [50, 51, 52]. As load cycles were accumulated, it was observed that most mechanical properties changed, but in particular the stiffness of specimens changed throughout the full duration of the fatigue tests; an equilibrium material stiffness was never reached. This behaviour was observed in elastomers containing reinforcing fillers. For carbon black filled EPDM test specimens, it was found that failure occurred when they reached approximately 76% of their initial stiffness (or complex tensile modulus E* was 76% of the initial tensile modulus), irrespective of the form or severity of the loads applied to the specimens during repeated cycling. Carbon black filled SBR test specimens failed in similar tests when they reached

approximately 71% of their initial stiffness. The results indicated that for non-strain crystallising elastomers there is a characteristic value for the material parameter (E*) that is reached at failure.

In respect of minimum load dependence (pre-stressing), results from the dynamic crack propagation tests on carbon black filled non-strain crystallising elastomers showed similar behaviour to that observed in the fatigue to failure tests. Increasing minimum loads at constant strain (displacement) amplitude, under both pulsed and sinusoidal excitation, decreased the crack growth rate of the carbon black filled rubber material. Thus it was argued that pre-loading can lead to higher service lives for parts produced from these materials. Unfilled EPDM and SBR test specimens showed no beneficial effects from pre-loading in either the crack propagation tests or the fatigue to failure experiments. As the normal failure observed during the fatigue to failure experiments was a sudden catastrophic crack when a certain level of stiffness (or modulus) was attained, it was assumed that these tests characterised the initiation process. It was thus, an important finding of the research that crack initiation and crack growth in rubbers displayed a similar dependence on test parameters. Furthermore, initiation and growth both appeared to be energy controlled processes in rubber materials.

Abraham determined that the parameter termed 'dynamic stored energy', when plotted against cycles to failure, provided a reliable predictor of fatigue life of EPDM samples and further that this parameter worked equally well for determining fatigue life in SBR samples. The value of dynamic stored energy is shown diagrammatically for one load / displacement curve in a cycle in Figure 1, as the area of the plot beneath the hysteresis curve where the minimum load in the cycle constitutes the lower boundary. The amount of energy available in the tensile pre-loading cycle, shown in red, is smaller than that in the load / displacement cycle with zero minimum load (no pre-load applied) shown in blue.

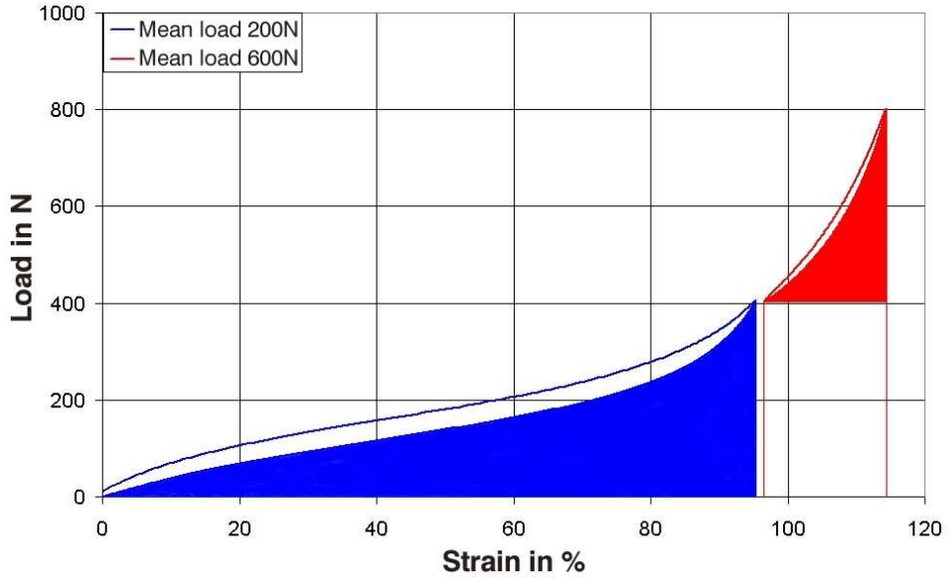


Figure 1. Diagrammatic representation of dynamic stored energy for two equal load amplitudes.

Wöhler (or S/N) curves for EPDM and SBR, where (log_{10}) dynamic stored energy was plotted as ordinate, are shown in Figures 2 and 3 respectively. Each graph includes data for tests on samples subjected to cycles with zero and non-zero minimum loads and different load amplitudes. Thus it can be seen that dynamic stored energy can provide a basis for reliable fatigue life prediction for non-strain crystallising rubbers. It was noted that for SBR, (log_{10}) of strain range plotted against (log_{10}) of cycles to failure could also be used to predict fatigue life for the material (Figure 4). However, it appears that dynamic stored energy offers a reliable parameter for predicting fatigue failure for non-strain crystallising rubbers that can be applied universally.

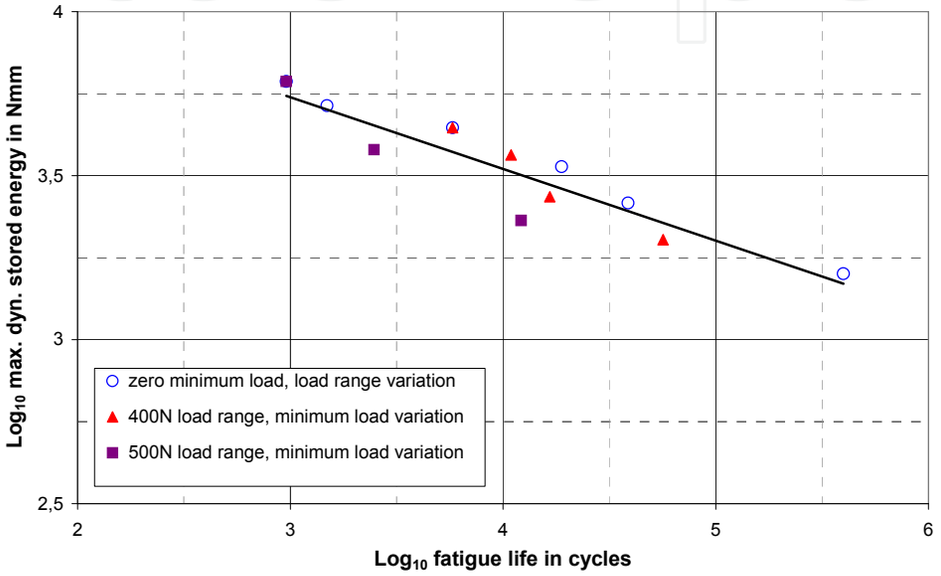


Figure 2. Log_{10} of maximum dynamic stored energy versus log_{10} of number of cycles to failure for filled EPDM for various load ranges and minimum loads.

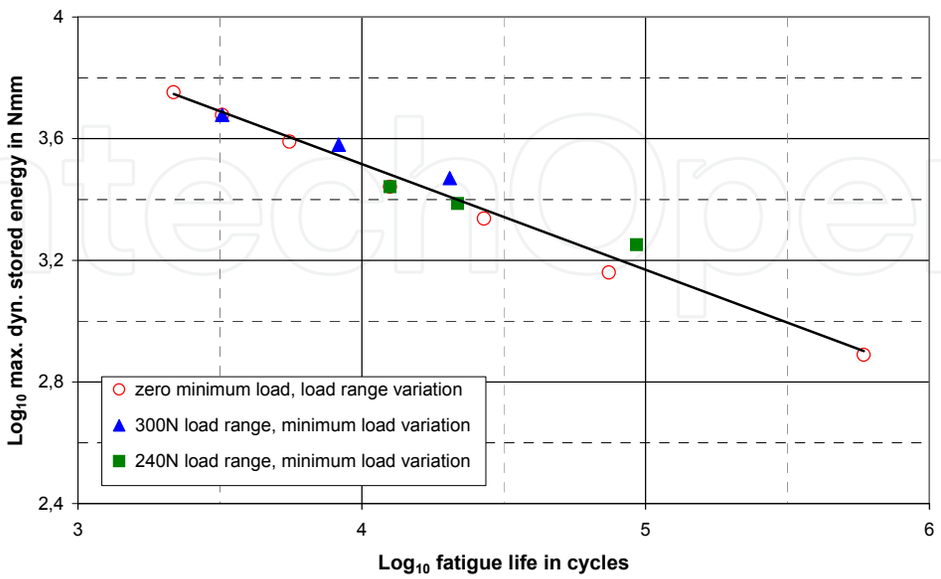


Figure 3. Log_{10} of maximum dynamic energy versus log_{10} of number of cycles to failure for filled SBR for various load ranges and minimum loads.

Figures 5 and 6 substantiate Abraham's third significant conclusion. They depict higher fatigue lives for test samples subjected to different levels of pre-stressing at different constant stress amplitudes, for EPDM and SBR respectively. This finding has prompted the hypothesis that pre-loading non-strain crystallising rubber components can enhance fatigue properties since less dynamic stored energy is available for higher stress ranges under such loading conditions.

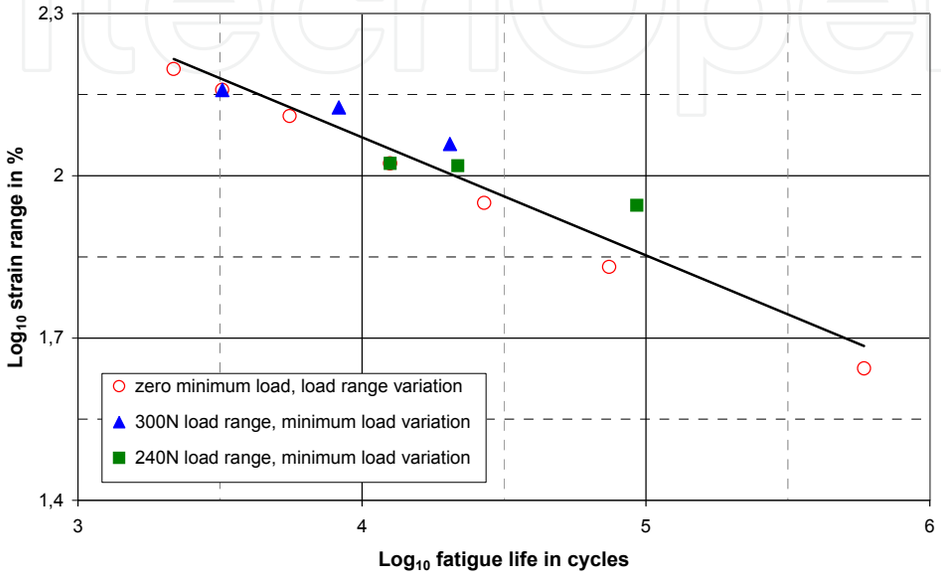


Figure 4. Log_{10} of the strain range against log_{10} of number of cycles to failure for filled SBR for various load ranges and minimum loads.

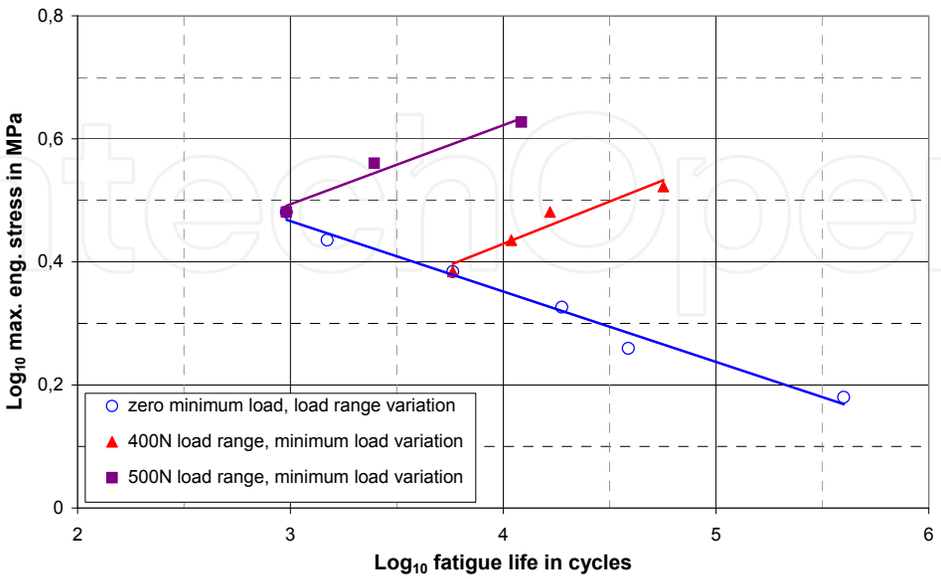


Figure 5. Log_{10} of the maximum engineering (nominal) stress versus log_{10} of number of cycles to failure for filled EPDM for various load ranges and minimum loads.

The data from all the tests show that the compounds underwent changes in physical properties throughout the load controlled cycles. The dynamic displacement induced an increasing amount of set as each test progressed. Typical hysteresis curves are shown in Figure 7. It is usual for the modulus of filled rubbers to decrease significantly during the first few cycles of a physical test as a result of stress softening (the Mullins effect) [53]. However, these fatigue tests indicated that E^*, as well as the storage modulus E', loss modulus E'' and loss factor (tan δ) decreased throughout the process to final fracture. In a typical fatigue test for which four cycles are shown in Figure 7, it is worth noting that no visible cracks were observed until 7449 cycles were reached and complete rupture occurred within approximately 250 cycles (at 7709 cycles). The same phenomenon was observed under less severe test conditions when test specimens failed after a few hundred thousand cycles.

The results of the fatigue testing suggest that elastomeric materials fail after a material specific loss in complex modulus E* is reached. This predictor seems to be a characteristic of each compound because it is independent of the applied loading. It does not depend on the load amplitude or the applied minimum load and so it is potentially a very important indicator for the maintenance of machines utilising elastomeric parts. The predictor allows us to assess the condition of rubber components easily and online and to replace them just before they fail. The influence of frequency and temperature on the residual stiffness predictor was not examined in this research, though it is well documented that fatigue resistance has a high dependency on these parameters. Moreover, pauses during dynamic testing and their role in the reconstitution of the filler network were not included in this research, so there is much still to be done.

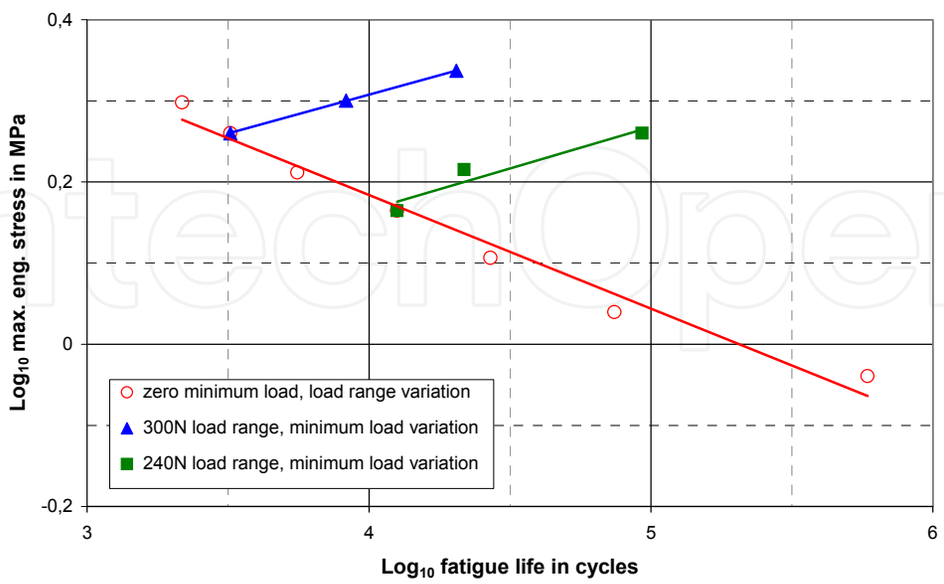


Figure 6. Log_{10} of the maximum engineering (nominal) stress against log_{10} of number of cycles to failure for filled SBR for various load ranges and minimum loads.

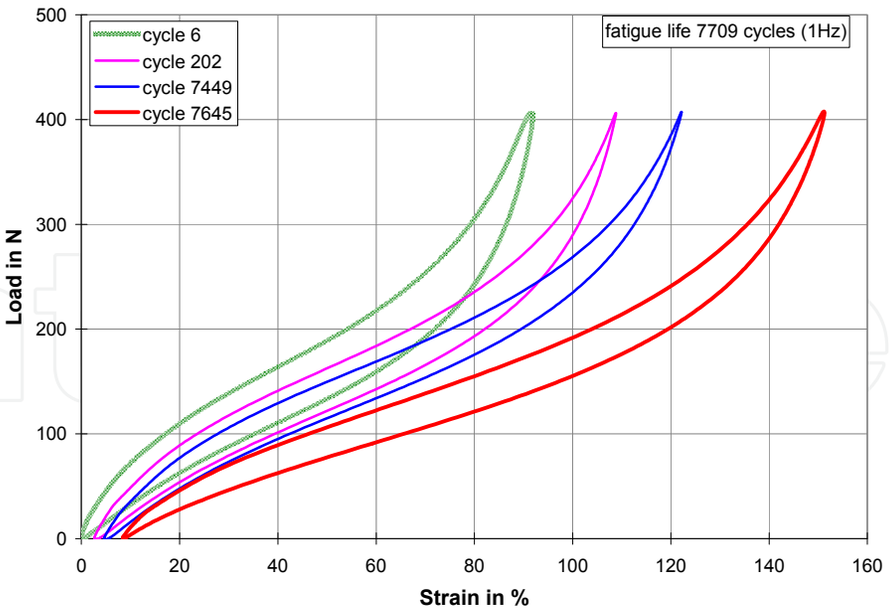


Figure 7. Hysteresis loops for a filled EPDM specimen during fatigue testing over a load range of 400N with no pre-load (1 Hz).

However, the research showed that, for the load amplitudes employed, the fatigue resistance of active carbon black filled non-strain crystallising EPDM and SBR rubber material increased when compressive or tensile preloads were applied. The increase in fatigue life resulted from the active filler and its filler-filler and filler-polymer interaction since this phenomenon did not occur in unfilled EPDM or SBR, where pre-loading reduces fatigue lives. This research showed that cyclic conditions from a minimum stress of zero are the most severe for active filled elastomers at these load amplitudes and also demonstrated that, like other solids, compression is less severe for elastomers than is tension.

The standard fatigue crack propagation testing described in the literature predominantly used displacement (strain) controlled tests. This is only applicable if service conditions under forced displacement are to be simulated. But most of the service conditions of elastomeric products are under load control and testing under displacement control would not provide the precision required. Clauss [54] compared load and displacement controlled fatigue tests. One result was that the stiffer (lower carbon black dispersion) materials failed much earlier under displacement control than softer materials. However, under load control both materials exhibited similar fatigue resistance. Clearly, for rubber the conditions of a laboratory simulation of fatigue life should be as close as possible to service conditions. If a rubber product is used under load control, then the testing should also be carried out under load control, otherwise the results can be misleading for two reasons. Firstly, stress softening occurs throughout the full life of the component. If the test was carried out under strain (displacement) control, less work would be applied in successive cycles and a pronounced modulus loss would not occur. Secondly, when materials of different stiffness are compared under displacement control, the stiffer material will always be more harshly tested than the softer material and so should fail earlier, because a higher stiffness will lead to higher stresses and strain energy densities.

Abraham's research questioned if the testing of crack growth is representative of the fatigue life of rubber components. Crack growth describes and compares approximately less than the final 5 % of the service life of a rubber product. The greater importance of deriving material or component data for the intact sample and to ascertain how long it remains intact is emphasised. Hence, the crack initiation stage represented in a Wöhler (S/N) curve is of more practical use to manufacturers than the time taken for a crack to propagate and bring about failure of a component. Thus, providing a reliable predictor of fatigue life is available, fatigue to failure tests should become the standard and relevant tests for Industry, even though they are more time consuming than crack propagation tests.

Abraham's research prompted the following questions;

i. Do non-strain crystallising elastomers exhibit a limiting value of complex modulus E* when cycled to failure under equi-biaxial loading?
ii. Do non-strain crystallising test specimens subjected to equi-biaxial loading have higher fatigue lives when they are pre-stressed ($\sigma_{min} \neq 0$)?
iii. Is there a limiting value of E* for swollen non-strain crystallising rubber samples?

Equi-biaxial bubble inflation was used to investigate these issues.

4. Equi-biaxial fatigue testing

4.1. The advantages of using the bubble inflation method

Consider two issues in respect of fatigue life prediction for elastomers and its simulation. Firstly, numerous phenomenological models for rubber used in Finite Element Analysis (FEA) are based on the James, Green and Simpson strain energy density function [55] which employs the even powered strain invariants I_1 and I_2. The formula for stress determined from the function is shown in Equation 6.

$$\sigma_1 = C_{10}\frac{\partial I_1}{\partial \lambda} + C_{01}\frac{\partial I_2}{\partial \lambda} + C_{11}\frac{\partial I_1\left(I_2-3\right)}{\partial \lambda} + C_{11}\frac{\partial I_2\left(I_2-3\right)}{\partial \lambda} + 2C_{20}\frac{\partial I_1\left(I_1-3\right)}{\partial \lambda} + 3C_{30}\frac{\partial I_1\left(I_1-3\right)^2}{\partial \lambda} \quad (6)$$

where C_{10}, C_{01}, C_{11}, C_{20} and C_{30} (MPa) are elastic constants determined from specific material test data

The significant contribution of the second strain invariant in bi-axial deformation is easily demonstrated. Consider the magnitude of the strain invariant I_2 and its derivative for biaxial deformation with respect to stretch ratio λ:

$$I_1 = 2\lambda^2 + \frac{1}{\lambda^4} \quad (7)$$

$$\frac{\delta I_1}{\delta \lambda} = 4\lambda - \frac{4}{\lambda^5} \quad (8)$$

$$I_2 = \lambda^4 + \frac{2}{\lambda^2} \tag{9}$$

$$\frac{\delta I_2}{\delta \lambda} = 4\lambda^3 - \frac{4}{\lambda^3} \tag{10}$$

So for even low values of C_{01}, C_{11} etc. terms become large for high deformations in the bi-axial load case. For example, with a biaxial stretch ratio λ of 2 and a typical value for C_{01} of say 0.04 MPa, the component of stress for the second term in the equation becomes

$$\begin{aligned} C_{01}\frac{\partial I_2}{\partial \lambda} &= C_{01}\left(4\lambda^3 - 4\lambda^{-3}\right) \\ &= 0.04\ \left(31.5\right) \\ &= 1.26\ MPa \end{aligned} \tag{11}$$

This value of stress alone is significant for a rubber-like material irrespective of the evaluation of the other terms.

The second issue requiring consideration is the amount of scatter present in fatigue to failure tests for rubber which is invariably large. The research carried out by Alshuth and Abraham *et al* [56, 57] on un-notched EPDM dumbbell samples generated Wöhler (S/N) curves to determine a reliable fatigue prediction criterion for this and other non-strain crystallising materials. Although, it was established that there was a relationship between the dynamic stored energy in successive stress-strain cycles and the number of cycles to failure, there were high levels of scatter in the experiments. This is typical of all fatigue tests of rubber compounds and it is believed that the scatter is a consequence of variations in flaw size at the failure cross-section. Subsequently, Abraham *et al* [58] conducted crack growth tests on EPDM single edged notched samples (SENs) and using Equation 5 correlated lives from these tests with those determined for un-notched dumbbell specimens. The flaw size in the dumbbells was controlled by evenly distributing glass spheres of constant diameter in the structure. It was found that the results from the fracture mechanics and Wöhler methods of prediction converged for samples containing glass beads of 203 μm in diameter, suggesting that cracks in the test material would emanate from naturally occurring flaws of this size. This allowed Abraham to control the amount of scatter in dumbbell fatigue tests, but at the expense of inducing unrepresentative early failures due to the severity of the flaws. Subsequent research into the prevalence of large flaws in samples of the same material was undertaken by Robin and McNamara [59] using tomography to establish the total number of large flaws in notched EPDM dumbbell specimens (shown diagrammatically in Figure 8) and the number of flaws in the critical region of a sample. Typically, it was found that 67 (N) flaws of 200 μm in diameter or greater, with an average volume of 0.394 mm^3, were present in a gauge volume of approximately 4770 mm^3. If the average volume of a large flaw is considered to be a single discrete volume, then the number of discrete volumes in the gauge volume was 12,107 (V_A) and the number of discrete volumes in the critical region (Figure 8) was 311 (V_B). The probability that critical flaws were absent from the critical region is given by:

$$\left(\frac{V_A - N}{V_A}\right)^{V_B} \tag{12}$$

Hence, for this analysis the probability equalled 0.178; therefore there was approximately an 18% chance of there being no large flaw in the critical region. The dumbbells were subjected to uniaxial cyclic loading and significantly on average one in every five to six samples exhibited an inordinately high fatigue life. This finding led to the hypothesis that notched samples had higher fatigue lives than un-notched samples due to the likelihood that flaws would often be absent from the vicinity of the stress concentration associated with the notch. Figure 9 shows an X-ray tomography image of a dumbbell sample with one large flaw (≈ 500 μm in length) close to the centre of the sample [60]. Interestingly, Kingston and Muhr [61] have recently published estimates of effective flaw sizes to initiate fatigue failure in uniaxial fatigue on parallel sided test-pieces for three materials; NR without carbon black, NR with 45 pphr N330 carbon black and SBR with 77 pphr N339 carbon black. For the latter two (rubbers containing carbon black), nominal flaw sizes at high strain rates (250%) were 209 μm and 219 μm respectively. The effective flaw size for the unfilled NR at this strain amplitude was nominally 67 μm. Effective flaw size diminished with reduction in strain amplitude for all three materials.

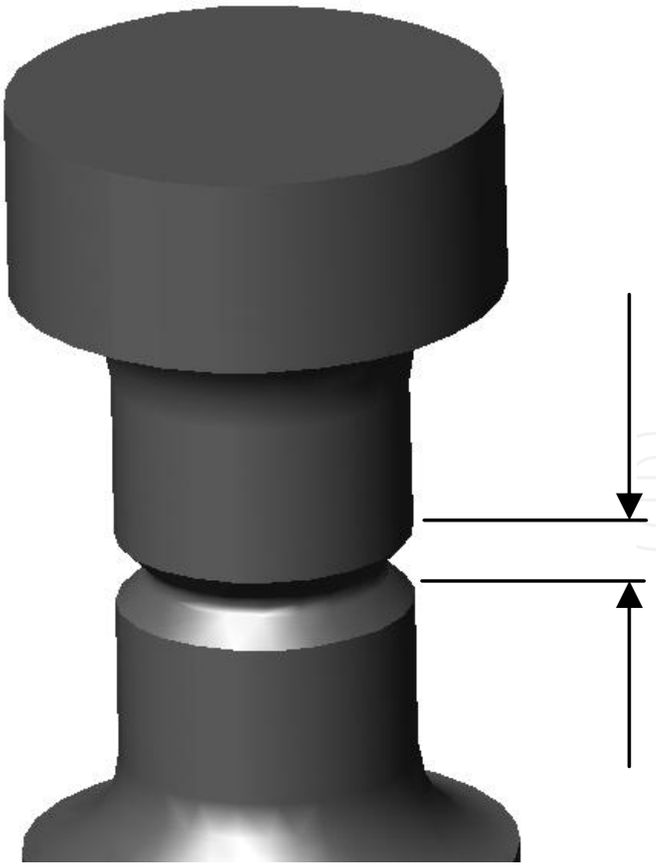


Figure 8. A diagrammatic representation of a dumbbell specimen. The volume of the critical region is indicated as that confined to the notch as shown.

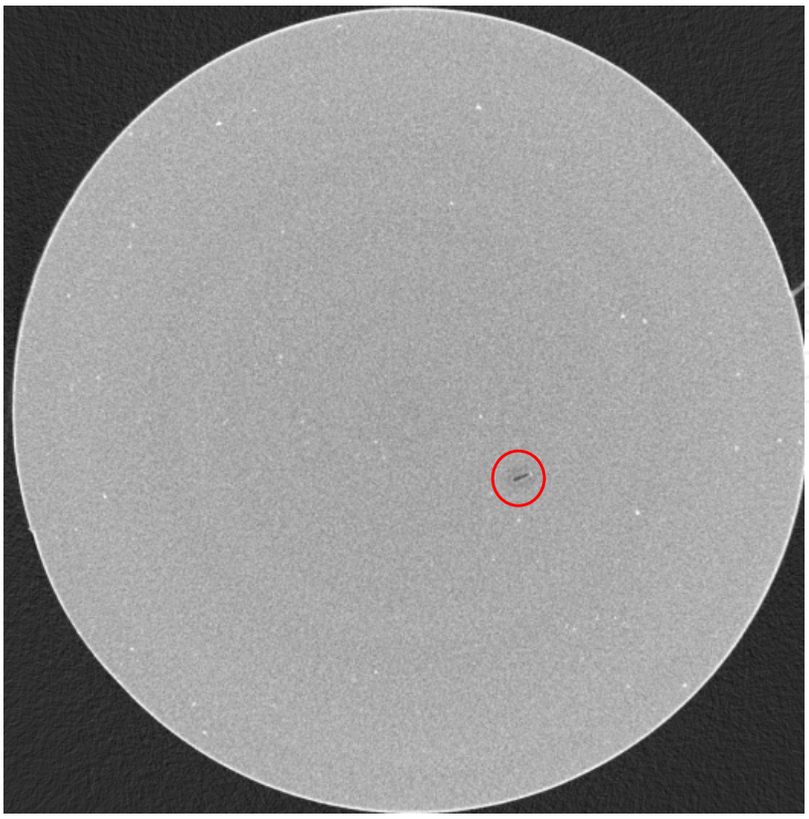


Figure 9. X-ray tomography image of a 15 mm diameter dumbbell sample showing imperfections of various sizes in one plane through the specimen. (A flaw of approximately 500 μm in length can be seen close to the sample centre. The image is reproduced from an analysis performed by S. Robin).

It is evident that two important questions are posed in relation to elastomer fatigue where dynamic equi-biaxial bubble inflation provides the solution; these questions are:-

i. How can fatigue tests be carried out on rubber samples that are representative of the multi-axial loading that components experience in service?
ii. How can fatigue to failure tests be performed on rubber specimens that do not produce results with high levels of scatter?

i. The first question is resolved using the bubble inflation method. For a circular membrane, clamped at the edge and subjected to inflation, the local deformations are a function of radius, from equi-biaxial at the pole to planar extension (approximating to pure shear) at the clamped radius. At the pole, the largest principal stresses (meridian stress σ_1 and hoop stress σ_2) are equal as shown in Figure 10, whilst the smallest principal stress (σ_3) is zero, normal to the outer surface.
ii. In a standard dog-bone equi-biaxial fatigue test-piece, failure can occur anywhere in the parallel gauge section of the specimen and so early fractures are common where a large flaw exists at some point in this section. Since most failures will occur at the point of highest principal stress (at the bubble pole) in an equi-biaxial bubble inflation test, this method has the advantage of reducing scatter in fatigue tests. If rarely, failure occurs away from the bubble pole, it is apparent that a large flaw is present at the point of failure and this test can be ignored.

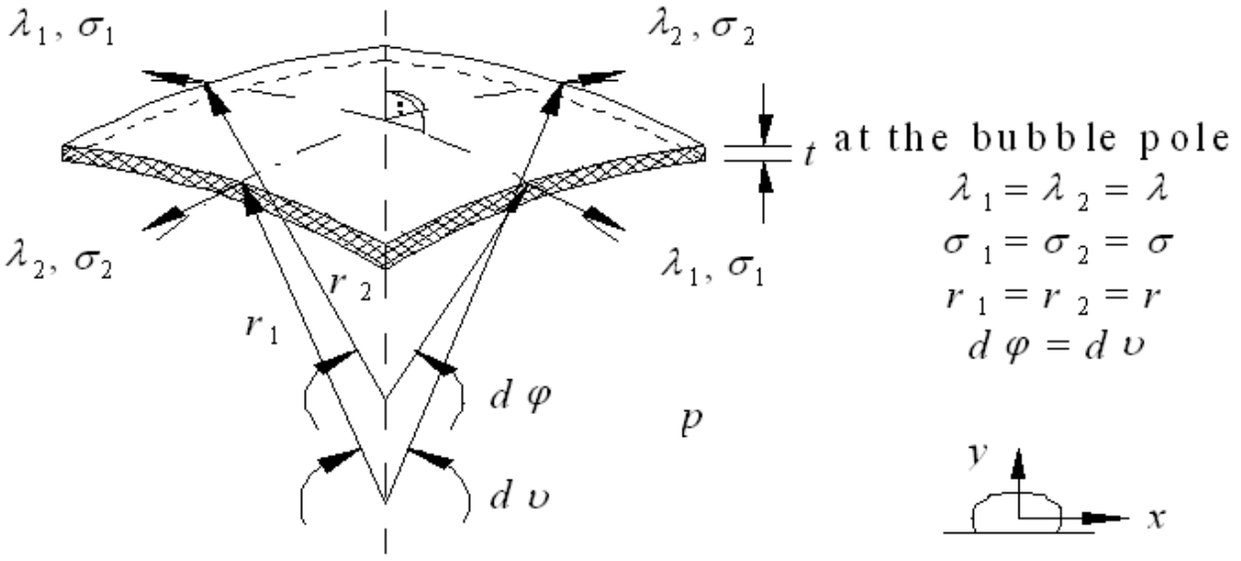


Figure 10. Membrane stresses at the pole of a bubble.

A typical stretch frame is shown in Figure 11. By comparison with the bubble inflation method, using stretch frames lead to the disadvantages of:

- High stress concentrations in the vicinity of the clamps
- Variation in stress distribution toward the specimen centre
- The small stretch ratios achieved result in stress amplitudes that either will not induce failure or alternatively make fatigue to failure tests inordinately long
- Large friction and inertia losses
- An inability to perform equi-biaxial creep tests.

4.2. Obtaining equi-biaxial stress-strain relations for rubber using bubble inflation

Bubble inflation has been used extensively in the past to study the hyperelastic behaviour of rubber [62, 63, 64, 65, 66, 67, 68, 69] and the research described here had its beginning in a project carried out in Robert Bosch GmbH. Johannknecht *et al* [70, 71, 72] pneumatically and hydraulically inflated nitrile rubber test samples to failure to determine material constants for hyperelastic FE analyses and also offered plausibility criteria for these constants [73]. Failures achieved by pneumatic and hydraulic static bubble inflation of Hydrogenated Nitrile Butadiene Rubber (HNBR) samples are shown in Figure 12. It can be seen that the fracture in the pneumatically inflated sample is far more severe than that in the hydraulically inflated sample. Bubble inflation is considered to comply with theory for thin shell structures subjected to pressure (membrane theory), in which bending stiffness is assumed to be negligible. For an ideal isotropic material and an axisymmetric set-up, the bubble contour exhibits rotational symmetry (as depicted in Figure 10). Johannknecht utilised images produced by two mutually perpendicular monochrome charge-coupled device (CCD) cameras to determine displacements at the bubble pole.

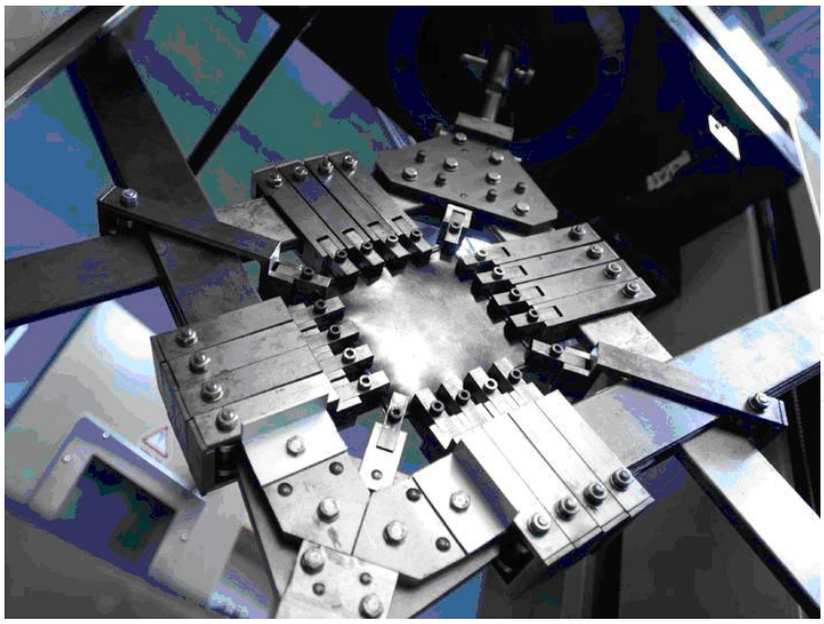
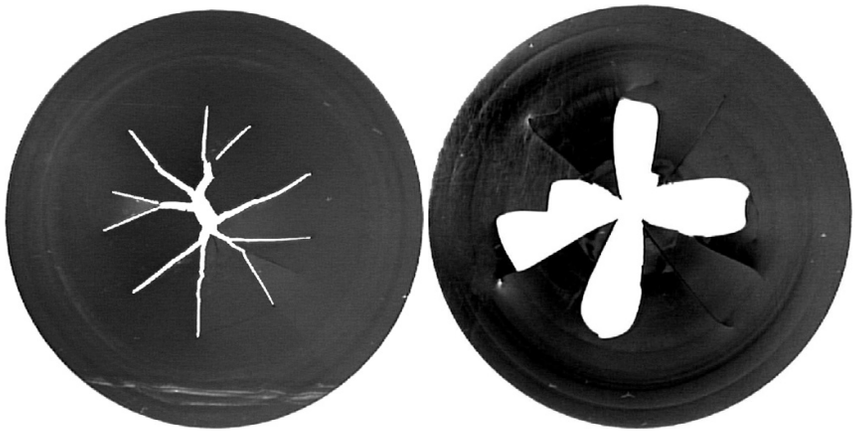


Figure 11. A stretch frame used for equi-biaxial loading of rubber specimens.



(a) (b)

Figure 12. Failure of statically inflated HNBR 50 mm samples, a) hydraulically inflated and b) pneumatically inflated

Using the simple expression for circumferential stress at the pole (σ), given in Equation 13, where P is the applied pressure, r the radius of curvature and t the specimen thickness, equi-biaxial stress-strain curves to failure were plotted that allowed material constants to be determined using the standard curve fitting procedures available in commercial FE software codes.

$$\sigma = P \cdot \frac{r}{2t} \tag{13}$$

Local stretch ratios at the pole can be determined using Equation (14).

$$\lambda = ((x_{cir} - x_{orig})/x_{orig}) + 1 \tag{14}$$

Where λ is the principal stretch ratio, x_{cir} is the circumferential point spacing at the bubble pole and x_{orig} is the original unstrained circumferential point spacing [70]. When the bubble height exceeds the radius of the inflation orifice, the bubble profile changes from spherical to elliptical which necessitated the calculation of an effective 'radius' at the bubble pole to allow engineering stresses to be computed. Murphy [74] showed that the formula for engineering stress σ_{Eng} had to be modified to include increased loading as a bubble enlarged (Equation 15). This meant that the relationship between engineering and true (Cauchy stresses) σ_{True} during dynamic bubble inflation was identical to that in uniaxial extension and equi-biaxial tension using stretch frames. Hence, the expression for Cauchy stress σ_{True} is as shown in Equation 16.

$$\sigma_{Eng} = P\left(r / 2t_o\right) \cdot \lambda \tag{15}$$

$$\sigma_{True} = P\left(r / 2t_o\right) \cdot \lambda^2 \tag{16}$$

where P and r are as previously defined and t_o is the unstrained sample thickness.

Unlike simple tensile and stretch frame testing, the total load acting on the specimen increases as the test progresses and the bubble expands under pressure.

4.3. Dynamic bubble inflation

Previously there was a dearth of research into dynamic bubble inflation [75, 76], although the method is capable of loading test-pieces in equi-biaxial tension for a large range of stress or strain amplitudes and allows the total number of cycles to failure to be recorded. Using the system advanced by Murphy [74] specimens were fatigued to failure and the resulting data when used in conjunction with other load cases, facilitated a full characterisation of fatigue properties for a particular elastomer sample subjected to complex loading. The characterisation of the equi-biaxial dynamic properties of EPDM was carried out in an initial programme to validate Abraham's findings for the uniaxial cyclic loading of non-strain crystallising rubbers [77]. However there are many difficulties associated with obtaining reliable fatigue data using the bubble inflation method. Consider the disparate requirements of determining fatigue life for specimens subjected to i) constant pressure amplitudes, ii) constant strain amplitudes iii) constant engineering stress amplitudes and iv) constant true stress amplitudes. Load case i), representative of a diaphragm in a machine working between set pressure limits, is the most easily achieved. The test-piece will grow continually throughout inflation / deflation cycles and be subject to stress softening and set. Constant strain amplitudes, load case ii), representative of the deformation at some point on a component like a belt, hose or drive shaft boot, require continual monitoring and control of specimen profile to retain an approximately equal deformation by varying the pressure limits. Load cases iii) and particularly iv) are representative of the majority of rubber components; auto exhaust hangers, tyre treads, engine mounts, etc. and require both continual monitoring of pressure and specimen profile as each parameter influences stress levels in subsequent cycles. Thus, to obtain

successive cycles at a constant engineering stress amplitude in bubble inflation, continually coordinating hydraulic, vision and control systems is essential. This is made complex by the need to continually adjust inflation pressure as the load experienced by the bubble surface increases with bubble growth due to the Mullins effect [53], but it is the large reversible deformations associated with rubber that make it so useful in all spheres of technology. Thus, characterising the material using true (Cauchy) stresses is far more relevant than using engineering stresses. In a conventional linear elastic solid, this distinction is unimportant because engineering stresses are virtually equal to true stresses as the materials normally only experience micro-strains.

Accordingly, Murphy *et al* [78, 79, 80, 81, 82] have developed a bubble inflation facility to produce reliable equi-biaxial fatigue data using a system similar to that employed by Johannknecht [70]. However, they were constrained to use hydraulic inflation and deflation as the lags induced in pneumatic systems were incompatible with cyclic loading. The system can also be used to determine static failure strength, stress relaxation, creep, stress softening and set for dynamic equi-biaxial loading. As stated, the initial impetus for the research was to determine if Abraham's findings [47] in uniaxial fatigue testing of non-strain crystallising rubbers were confirmed for biaxial loading. Very little research had been carried out previously using dynamic bubble inflation of rubber, though Bhate and Kardos [75] used bubble inflation to study high frequency vibrations in elastomers and Hallett [76] studied equi-biaxial rubber fatigue without integrating the systems essential to allow full control of the tests. Hence, unlike the previous investigations, the hydraulic system was integrated with control and vision systems to allow cycling at constant amplitudes of pressure, strain and stress and offered ready access to test results. Murphy applied a system for tracking the displacement of a row of dots at the bubble pole to record circumferential displacement using two CCD cameras, but unlike Johannknecht, he achieved this objective with a camera placed on the vertical axis above the bubble pole and another inclined at 45^0 to the vertical axis. The system configuration is shown in Figure 13. An inflated test sample is shown in Figure 14.

Fatigue to failure tests were carried out on an EPDM rubber of 70 Shore A hardness, containing 110 pphr low activity carbon black with 70 pphr softener added. The bubble specimen consisted of a rubber disc of 50 mm and a thickness of 2 mm cut from an EPDM sheet, the inflating orifice was 35 mm in diameter. The first tests were carried out at constant pressure amplitudes and a typical stress-strain plot showing cycles selected at intervals in a fatigue test is given in Figure 15. Thereafter, the system was developed to facilitate repeated cycles under constant engineering stress amplitude control, using the relationship $\sigma_{Eng} = PR\lambda_1/2t_o$. Cycles selected at intervals in a typical test are shown in Figure 16.

Figure 17 depicts selected cycles for a fatigue test on an EPDM sample (zero minimum stress) under constant stress control and shows that stress softening continues for the duration of a fatigue test, as was observed by Abraham in uniaxial dynamic testing of the same material.

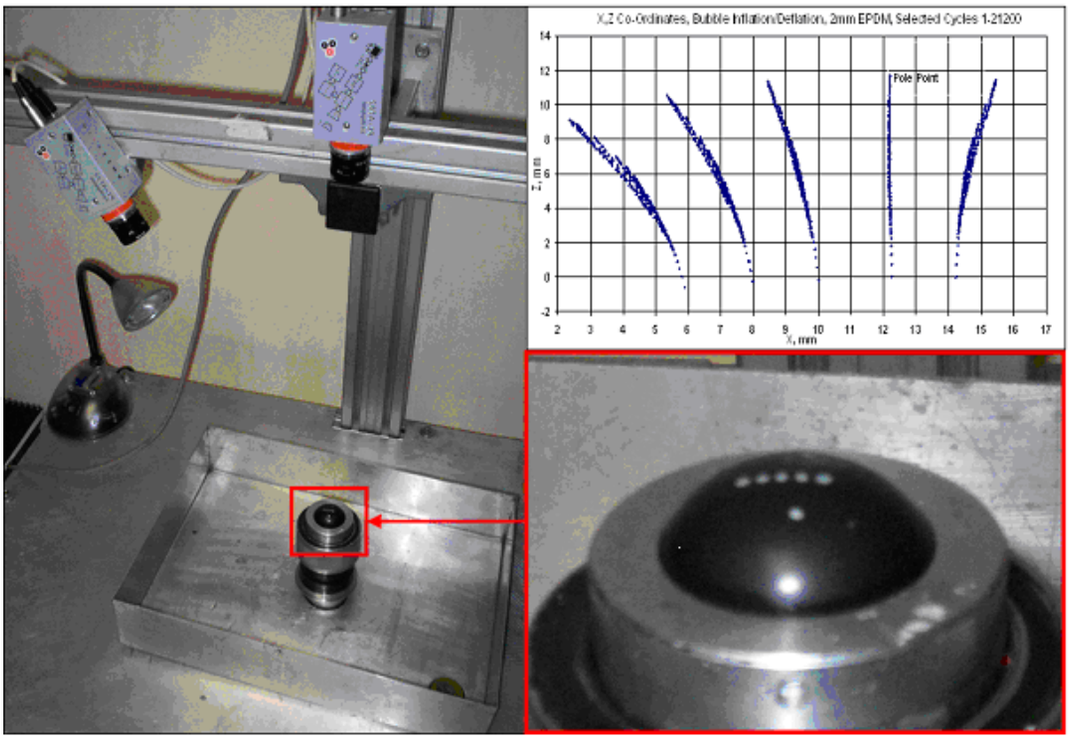


Figure 13. The final configuration of the equi-biaxial bubble inflation test system.
The graph depicts the tracking of the displacement of centres of dots at the pole of the bubble.

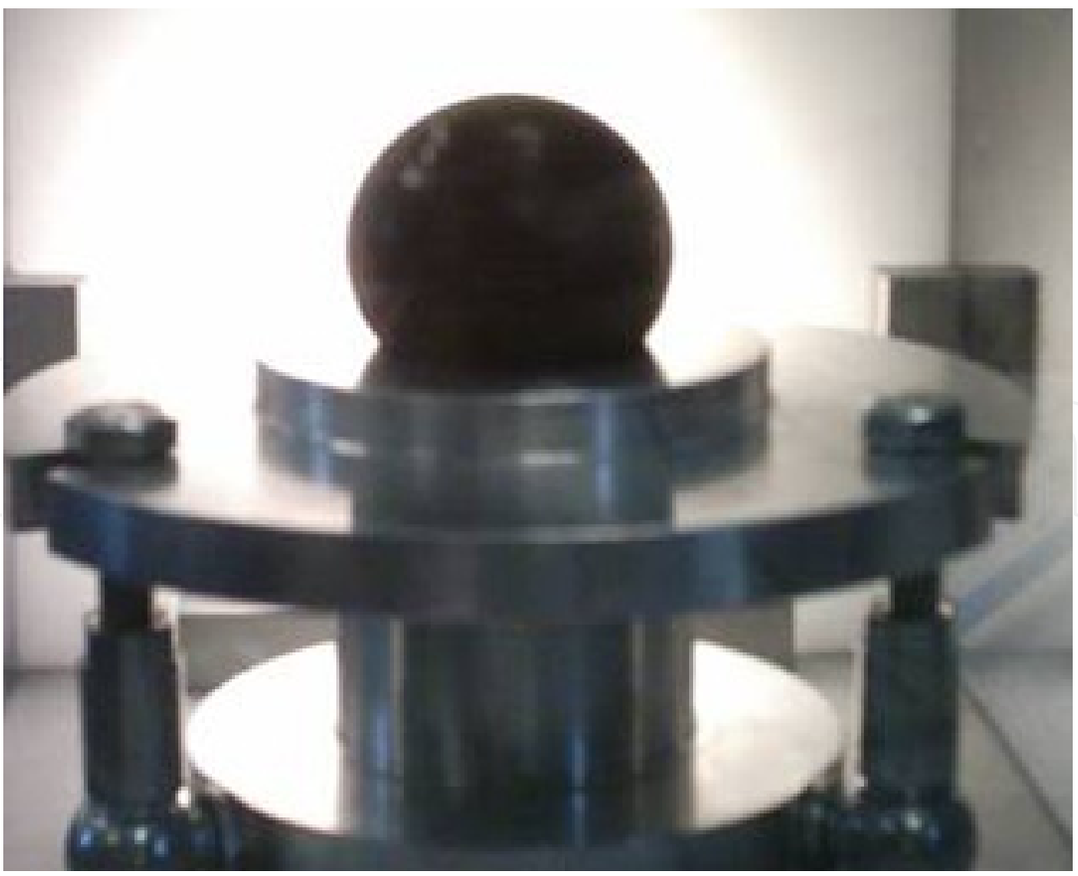


Figure 14. An inflated EPDM test sample

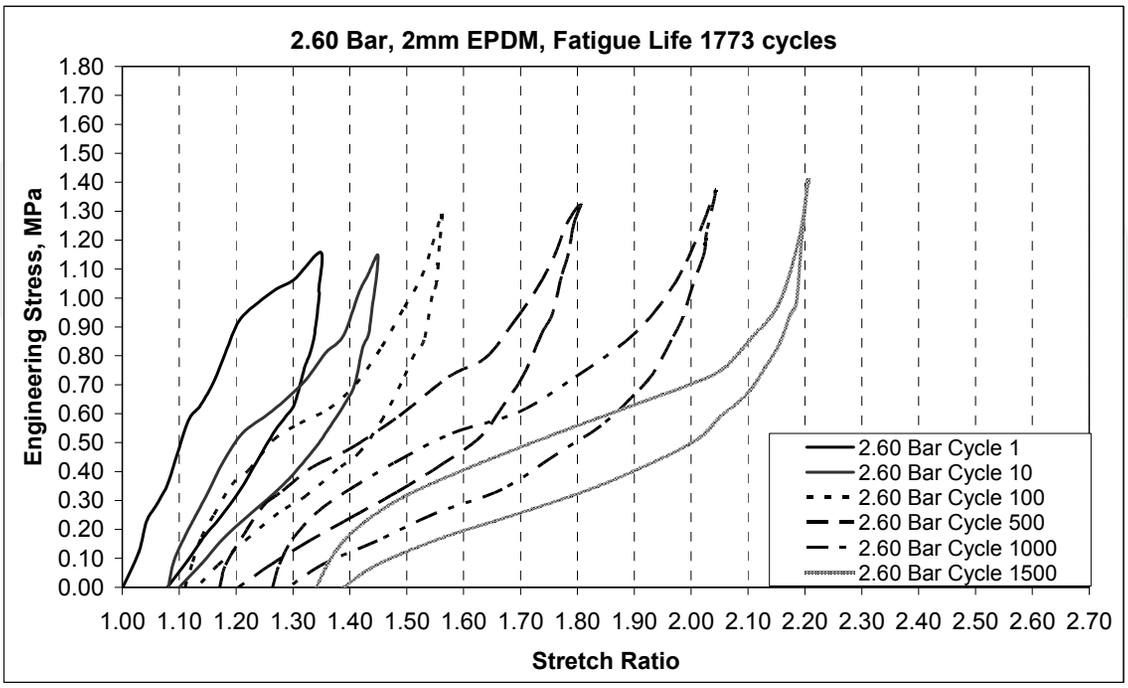


Figure 15. 2 mm thick sample cycled between constant pressure limits ~ selected cycles.

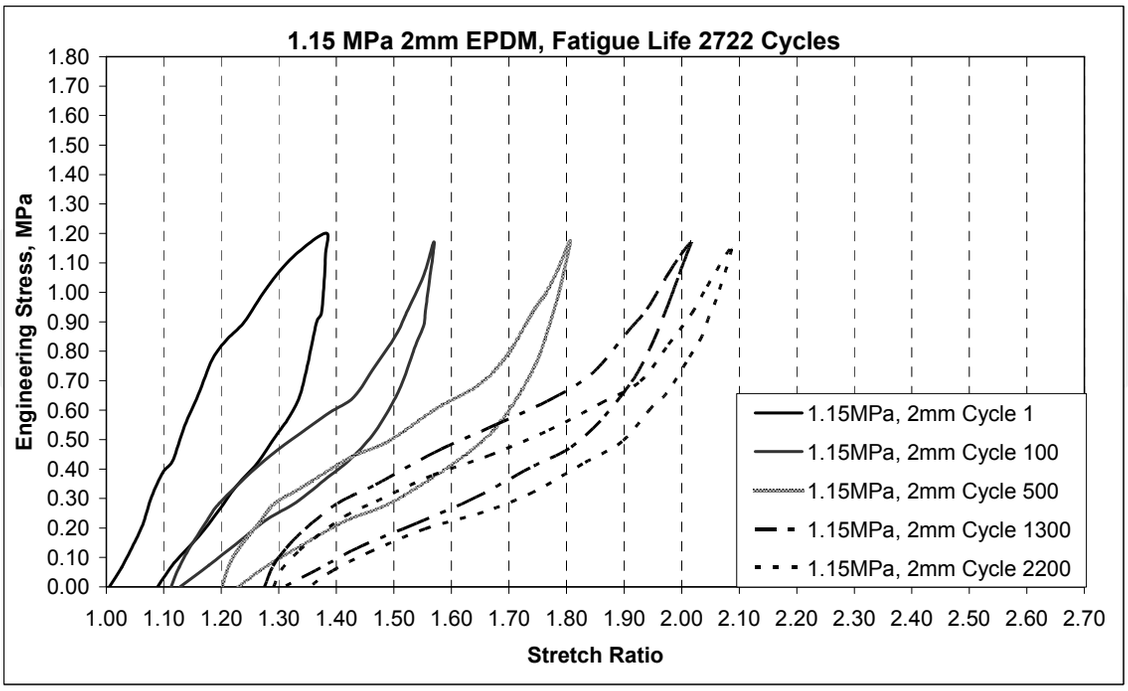


Figure 16. 2 mm thick sample cycled between constant engineering stress limits ~ selected cycles.

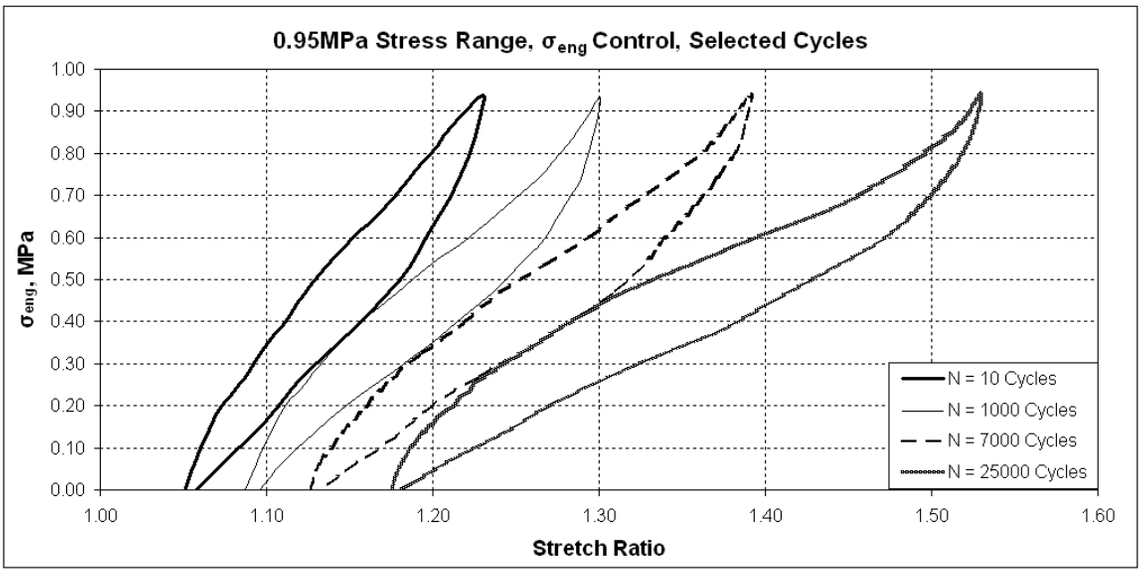


Figure 17. Hysteresis curves for selected cycles in a fatigue test on an EPDM sample.

Fatigue testing using constant engineering stress amplitudes and a non-zero positive minimum pressure did not definitively align with Abraham's observations for uniaxial pre-stressing of EPDM samples. In general, some increase in fatigue strength was observed with pre-stressing for higher pressure amplitudes, but not for smaller amplitudes. The effect of pre-stressing in dynamic equi-biaxial fatigue of EPDM shows that just below the high damage region of loading, increases in fatigue life were exhibited. It is apparent that the fatigue lives of samples cycled at higher constant equi-biaxial stress amplitudes with pre-stressing were greater than for samples cycled to the same stress amplitudes with zero pre-stressing. However, this effect is only exhibited for these high pre-stress levels as depicted in Figure 18. Figure 19 illustrates diagrammatically the variation in the effect of pre-stressing with changing engineering stress amplitudes and also highlights the relationships between the various loading regimes. Reducing dynamic stored energy due to pre-stressing in a loading cycle has less influence on the total dynamic stored energy available for lower maximum cyclic stresses and increases in stress (or pressure) ratio R for a material being tested, where:

$$R_{ratio} = \sigma_{min} / \sigma_{max} \left(\text{also } \mathrm{P_{min}} / \mathrm{P_{max}}\right) \tag{17}$$

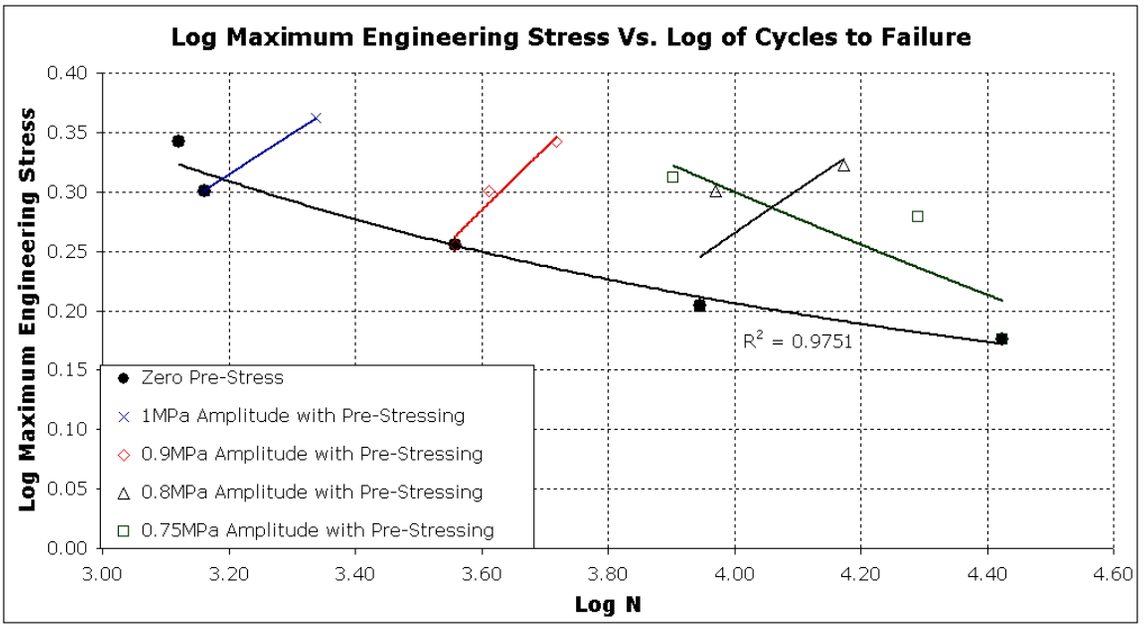


Figure 18. S-N curve for EPDM samples with and without pre-stressing, using $\sigma_{Eng} = P\ R\ \lambda_1/2\ t_o$ control.

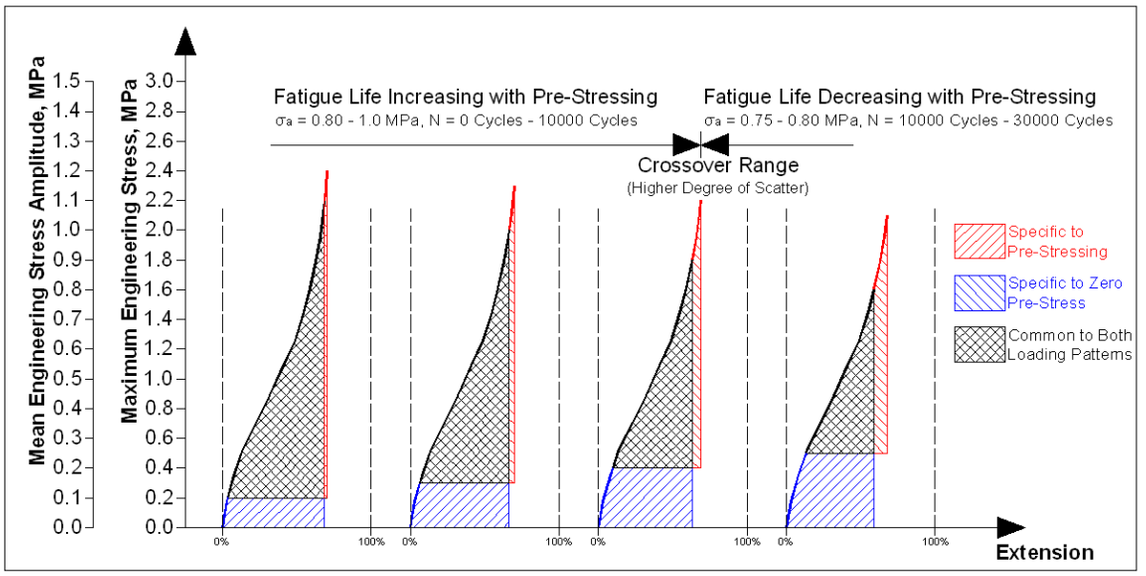


Figure 19. Effect of dynamic stored energy due to pre-stressing on fatigue life.

A point was reached below which the contribution of the stored energy solely attributable to the pre-stressing was insufficient to increase fatigue life and in fact, as the test programme continued, reduced fatigue lives were recorded for samples under pre-stressed conditions with lower maximum engineering stresses.

4.4. Equi-biaxial fatigue of elastomers subjected to swelling

There have been few investigations of the dynamic behaviour of rubber under the influence of oil swelling [83, 84, 85, 86] although swelling of elastomers has been comprehensively studied under conditions of static loading. All rubber swells to some degree in oil, but the

amount of swelling can be estimated for any oil-rubber combination if the solubility parameters Δ for both components are known. If the square root of the difference between the solubility parameters of the rubber and the oil is less than 1, as in Equation (18), then the rubber will swell appreciably in that oil [87]. To control the level of oil swell in elastomers it is practical to use hydraulic fluids where the properties have been pre-determined and can be used as a reference. Difficulties arise in precisely determining the solubility parameter of a fluid when it consists of two or more fractions. However, the solubility parameter for a hydraulic fluid can be estimated in experiments from other chemical properties which are readily available (e.g. the aniline point of the oil) and an empirical relation between the solubility parameter and the aniline point of the oils under test can be determined [88].

$$\left(\Delta_1 - \Delta_2\right)^{\frac{1}{2}} < 1 \tag{18}$$

The effect of oil swelling on the fatigue life of EPDM under conditions of equi-biaxial cyclic loading using dynamic bubble inflation was studied by Jerrams *et al* [49] and the research project set out to:

1. Determine if fatigue strength reductions due to swelling in rubber specimens loaded equi-biaxially were consistent with strength reductions in samples subjected to uniaxial tests to failure.
2. Create equi-biaxial Wöhler (S-N) curves for a range of rubbers swollen in different media in tests conducted at constant stress amplitudes.
3. Establish relationships between cycles to failure and dynamic modulus and stored energy.
4. Offer predictors of fatigue life for dry/swollen specimens subjected to equi-biaxial fatigue.

An EPDM rubber of 70 Shore A hardness, cross-linked with sulphur and containing low activity carbon black was used in the experimentation. The samples were 50 mm in diameter and prior to testing, had a thickness of 2 mm. Unconditioned samples were clamped and dynamically inflated and deflated through a 35 mm diameter orifice for the bubble inflation tests. The fatigue properties were initially considered for dry EPDM samples that had been subjected to ten loads cycles to condition them.

The degree of cross-linking of the EPDM material and hence its modulus is related to swelling potential by the Flory-Rehner Equation:-

$$\text{-ln}\left(1 - V_2\right) + V_2 + XV_2^{\,2} = \left(V_1 / \upsilon M_c\right)\left(1 - 2M_c / M\right)\left(V_2^{\,1/3} - V_2 / 2\right) \qquad \text{[89](19)}$$

where V_2 is the volume fraction of polymer in the swollen mass, X is the Flory-Huggins interaction parameter, V_1 is the molar volume of the solvent, M_c is the average molecular mass between crosslinks and M is the primary molecular mass.

Three different sets of EPDM samples were tested; the dry specimens and those swollen in two different ASTM reference oils,

IRM 902 and IRM 903. Specimens were subjected to varying degrees of swelling in reference mineral oils and fatigued at constant engineering stress amplitudes [90]. The reference oils used for swelling the EPDM had known aniline points, allowing the determination of rubber-oil compatibility. The silicone based oil used as the inflation fluid for fatigue testing was selected to minimise the amount of additional swelling during cycling. The samples were cycled between zero and predetermined maximum stress values. Wöhler (S-N) curves were produced for dry and swollen specimens and the changes in complex elastic modulus E* and dynamic stored energy were determined. Specimen fractures were observed using SEM. As in the equi-biaxial bubble inflation fatigue tests previously described, the specimens had a pattern of dots applied to their surface. The deformation of this pattern during inflation and deflation was recorded by the optical system previously specified [74], allowing correlation to a specific engineering stress value at the bubble pole. From ASTM standards for rubber-liquid compatibility, the reference oil IRM 903 was chosen as the most appropriate oil for high swelling of EPDM. Its aniline point was determined and compared with the solubility parameter of the EPDM to allow rubber-liquid compatibility to be gauged. Also, using reference oil, IRM 902, which imparts medium swell effects, allowed the influence of variation of oil solubility on rubber properties to be investigated [91]. Specimens were immersed in the reference oil at 100 °C for one hour. After removal from the hot oil the samples were cooled in oil at ambient temperature for a short period, before being dried and weighed. An average swelling ratio Q was calculated for the samples, where *Q* was expressed as,

$$Q = \frac{W_s}{W_d} \tag{20}$$

W_s is the weight of the swollen elastomer sample and W_d is the weight of the dry elastomer before swelling. A swelling ratio of 1.10 (10% increase in mass) was calculated for the EPDM swollen in IRM 903 and a ratio of 1.042 (4.2% increase in mass) for the EPDM swollen in IRM 902. EPDM specimen sets (Dry, 10% Swell, 4.2% Swell) were then cycled hydraulically between pre-set maximum and zero minimum engineering stress limits using the silicone based oil as the inflation medium. In general, fatigue tests were carried out at frequencies of 1 Hz to minimise any potential for samples to degrade due to heat build-up during cyclic loading [48]. However in bubble inflation tests there can be minor exceptions to this practice as it is essential to consider pressure or stress amplitude in combination with frequency to avoid thermal degradation. To maintain a constant maximum engineering stress in each cycle, the pressure set-point was adjusted continually throughout testing. S-N curves were produced to allow comparison of the fatigue lives of the dry and swollen rubber samples. The plot of stress amplitude (σ_a) versus cycles to failure (N) for all three specimen sets is shown in Figure 20.

As anticipated, the unswollen specimens had greater fatigue resistance than the swollen samples. The fatigue life of the material was reduced proportionally to the degree of swelling. The fatigue behaviour of the three specimen sets was subsequently analysed in respect of the complex elastic modulus, E* (as previously defined). Plots showing the

decrease in modulus E* of the samples with the accumulation of cycles at a stress amplitude of σ_a = 1MPa for the three sample sets are shown in Figure 21. (The three dashed curves represent results of FE simulations for the three material sets).

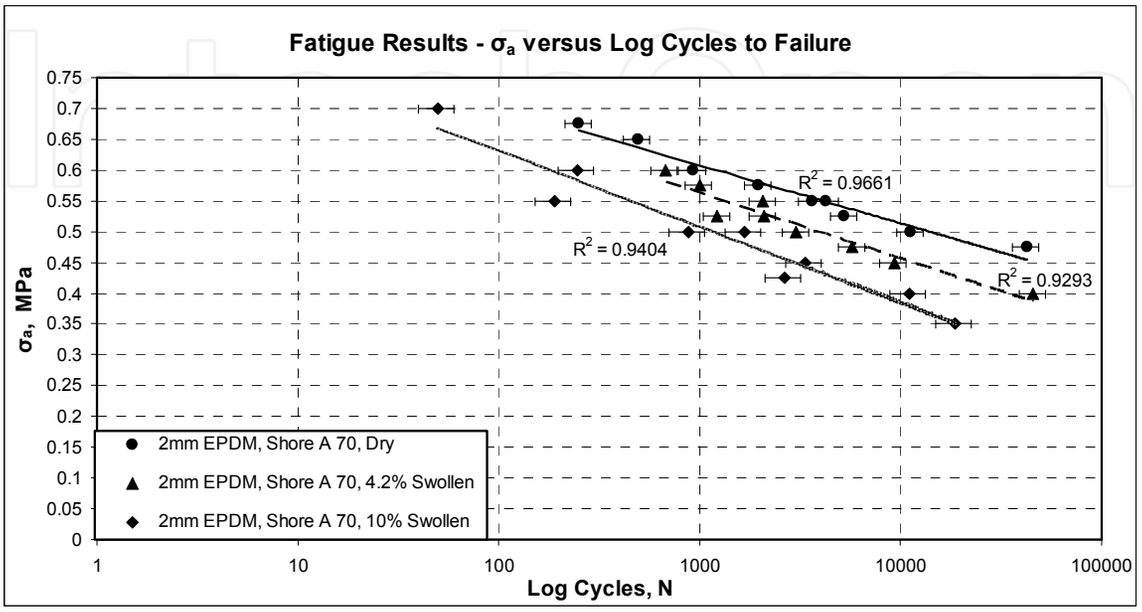


Figure 20. Plot of stress amplitude versus $\log_{10}$ cycles to failure for dry and swollen specimens.

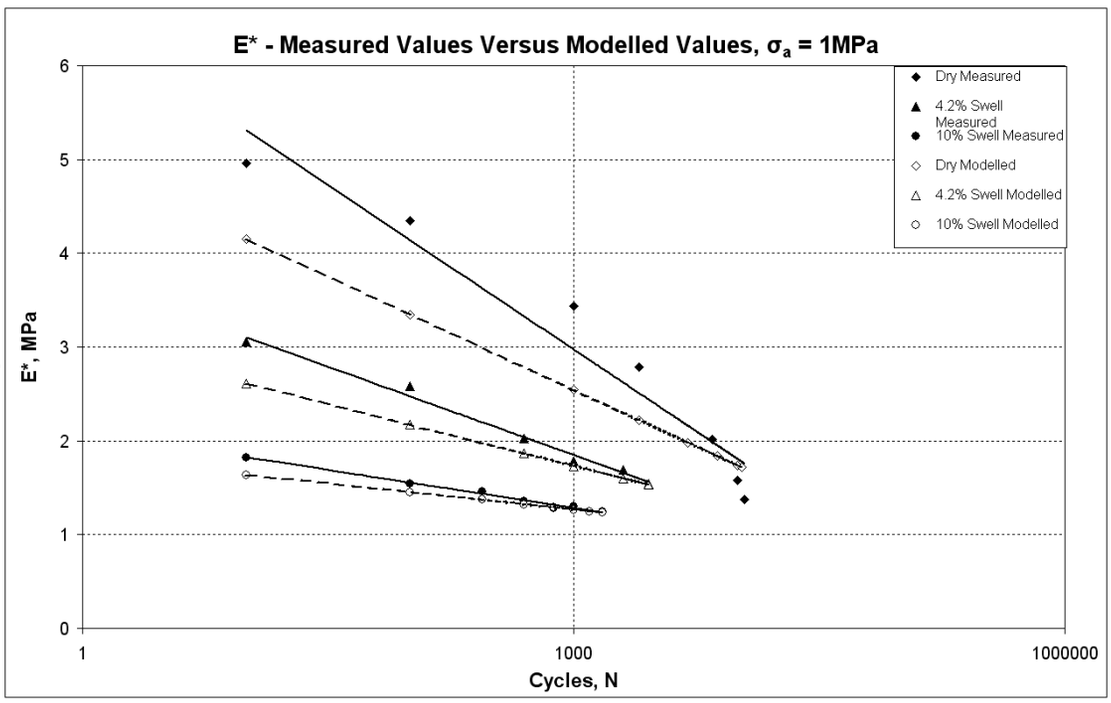


Figure 21. E* versus cycles $\log_{10}$N for dry, 4.2% and 10% swollen specimens at σ_a = 1MPa.

It was noted earlier that in tests carried out by Abraham, [47] it was found that for a given material, failure consistently occurred after a specific loss in complex modulus E*. This predictor, termed E^*_{res} can be represented as:

$$E^*_{res} = \left(E^*/E_{con}\right) \times 100\% \tag{21}$$

where E_{con} is defined as the modulus of the material after ten conditioning cycles. The dry and swollen specimens subjected to equi-biaxial cycling were analysed using this approach, where the percentage value of E^*_{res} versus cycles was plotted up to 95 % of the fatigue life of the specimen. A plot of the decrease in E^*_{res} (as a percentage of E_{con}) for the dry EPDM is shown in Figure 22. E^*_{res} was found to have an average value of 33% ±10% of its original value at 95% of the fatigue life of each dry specimen. The 4.2% and 10% swollen specimens had values of E^*_{res} of 50.5%±10% and 60.1%±5% at 95% of specimen life, respectively.

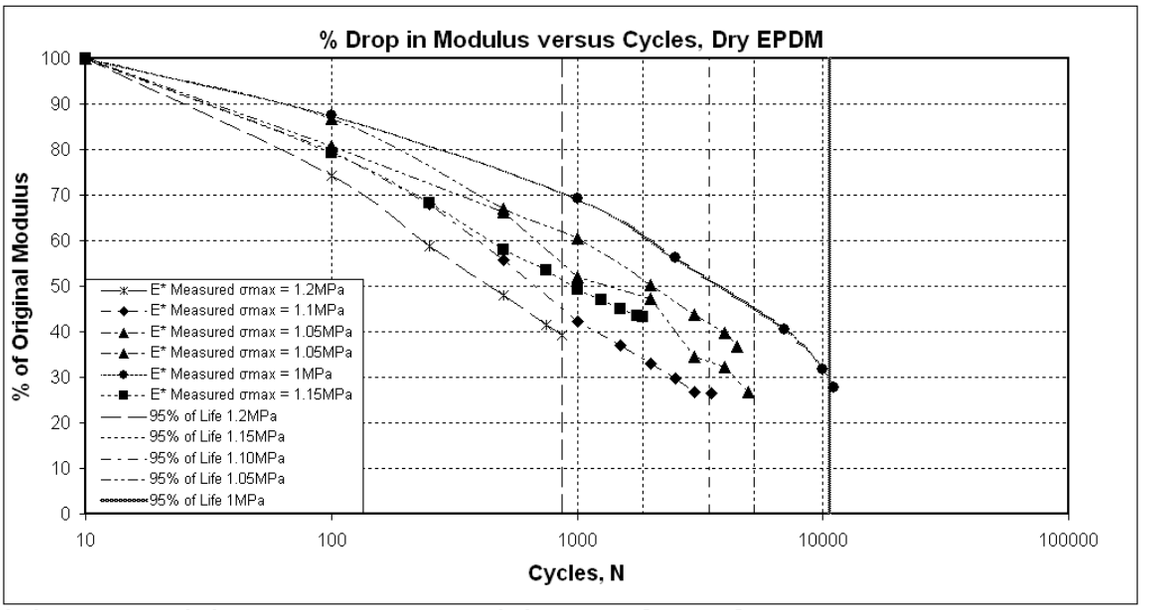


Figure 22. E^*_{res} versus $\log_{10}$ cycles N for dry EPDM for five different stress amplitudes.

The moduli (E*) for the dry and swollen samples at failure were studied by comparing the dry and the two swollen specimen sets at similar stress amplitudes. The trends for each specimen set are shown over a range of stress amplitudes in Figure23.

There is an average E^*_{res} at failure of 33% ±10% for these sets of specimens over four different stress ranges. By knowing the initial modulus E^*_{con} for the dry specimens, an approximation of the failure modulus for the swollen test-pieces can be determined. At a stress amplitude of 1MPa, comparison can be made between all three sample sets in respect of the decrease in specific modulus. Analysis of the value to which E^*_{res} decreases for each sample type at a stress amplitude of σ_a = 1MPa, with E^*_{con} taken as the modulus of the dry EPDM after ten conditioning cycles, suggested that E^*_{res} at failure fell within the 33% ±10% range for each of the three specimens. The dynamic stored energy during cycling of the

three sample sets was also evaluated. Previous analyses of uniaxial test data for EPDM found good correlation between the dynamic stored energy in the specimen versus the cycles at failure and its use as a plausible fatigue life predictor was proposed [51-52]. Stress-strain measurements were made periodically throughout the equi-biaxial dynamic tests. The dynamic stored energy in a cycle was subsequently calculated for the specific cycles measured. After conditioning, the dynamic stored energy increased linearly when plotted against cycles to failure, confirming that using this parameter provides a plausible predictor of fatigue life for elastomers, irrespective of the degree of swelling present in the material. The plots of dynamic stored energy to failure versus $\log_{10}$ cycles for the dry EPDM over a range of stress amplitudes are shown in Figure24 and the graphs of dynamic stored energy versus $\log_{10}$ cycles to failure for all three material sets are shown in Figure 25. At similar stress amplitudes, the dry EPDM samples had higher dynamic stored energy at failure than the swollen specimens, with the 10% swollen rubber having the lowest dynamic stored energy for a given stress amplitude. As would be expected, this result is due to a reduction in stiffness with increasing levels of swelling.

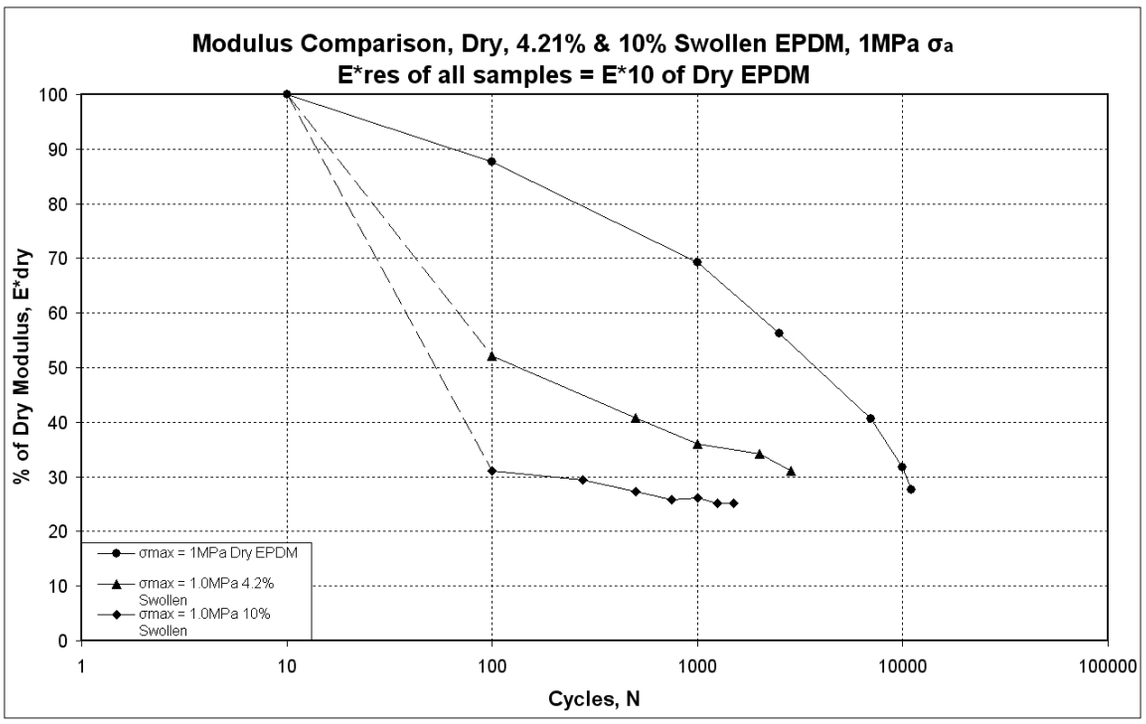


Figure 23. E^*_{res} expressed as a percentage of E^*_{con} versus $\log_{10}$ cycles N for dry and 4.2% and 10% swollen EPDM for different stress amplitudes.

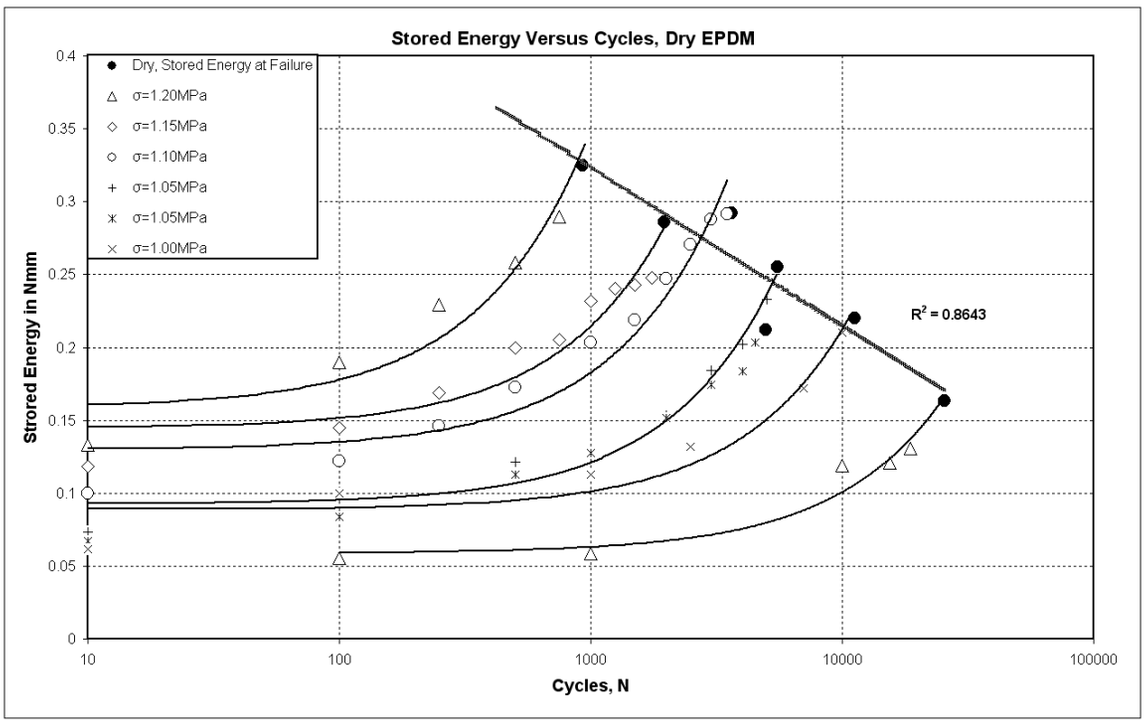


Figure 24. Dynamic stored energy versus $\log_{10}$ cycles to failure for dry EPDM samples

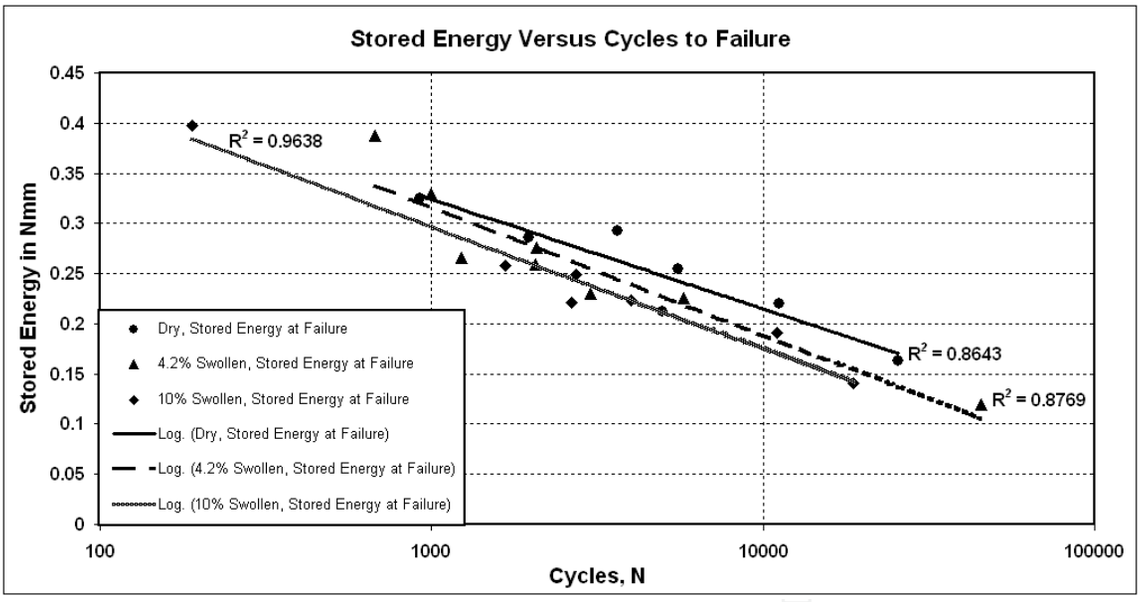
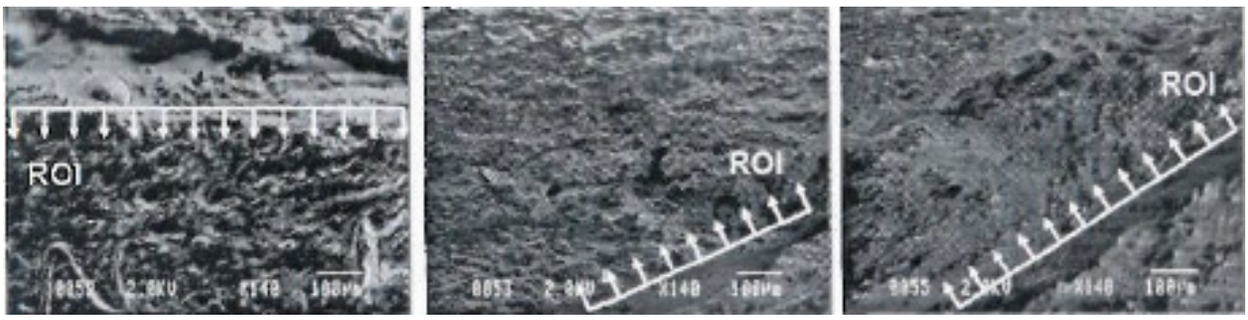


Figure 25. Plot of Dynamic Stored Energy versus $\log_{10}$ cycles to failure for the three specimen sets.

The surface morphology of the fractures for each sample set was observed. The fracture surfaces of the dry samples were analysed using SEM. A magnification factor of X400 at 2.0 kV was used to view failure surfaces. For low lives of less than one hundred cycles, the failure mode was similar to that observed for the fracture surfaces of the material from a static inflation test to destruction. The surface morphology was fibrous in nature and in some instances showed delamination at the failure surface. Failures that occurred beyond 100 cycles showed clear evidence of crack propagation and subsequent rupture. Cracks

propagated predominately in the bubble pole region. This behaviour was common to both the dry and swollen specimens. SEM images of the surface morphologies of the specimens at stress amplitude of 1 MPa are shown in Figure 26. In the dry samples there is a coarser failure surface at lower cycles than for failures at higher cycles. Previous research indicated that the surface of the dry samples exhibited blunt tearing, while the surfaces of swollen test-pieces indicated sharp tearing [75]. SEM images from this study confirmed these observations, where the blunter surfaces of the dry specimens were in stark contrast to the smoother surfaces of the swollen test-pieces. This blunt tearing was attributed to greater polymer filler interaction in the dry material, as the material showed higher toughness for equal values of applied stress. The SEM imaging suggests that the swollen failure surfaces 'flow' more readily over one another than those of the drier specimens.



Dry **4.2% Swollen** **10% Swollen**

Figure 26. SEM Imaging of specimen fracture surfaces, σ_{eng} = 1 MPa (ROI = Region of interest).

Flaws were more abundant in the swollen material. As the flaws were potential stress raisers, the probability of crack growth being initiated at them would be high and the areas around the flaws would tend to have a lower complex modulus than other points in the network.

5. Conclusions

Using load controlled uniaxial cyclic deformation of dumbbell specimens, Abraham *et al* [47] correlated fracture mechanics and SN curve approaches for determining fatigue life in non-strain crystallising rubbers. In subsequent analyses they were able to show that failure in fatigue would ensue from flaws of 200 μm or more in length if such flaws were in the critical region of the loaded specimen. By applying tomographic techniques, McNamara *et al* [60] were later able to confirm the presence of flaws of this magnitude in standard rubber samples and account for the large scatter in elastomeric fatigue tests by highlighting the possibility of these flaws occurring on critical sections in a test-piece or component. Abraham's research resulted in three other key findings in respect of fatigue resilience under uniaxial loading in amorphous elastomers. These can be summarised as:

i. Fatigue life can be improved by pre-loading these materials.
ii. 'Dynamic stored energy' can be used as a basis for predicting fatigue life
iii. There is a limiting value of complex elastic modulus E* below which fatigue failure can be anticipated.

These findings prompted numerous questions:-

a. Will the influence of pre-loading be significant under more complex loading regimes?
b. Can 'dynamic stored energy' be used as a predictor of fatigue life for multi-axial loading of rubber samples?
c. Is there a limiting value of E* that is applicable for non-strain crystallising rubbers loaded biaxially?
d. Can the dynamic stored energy criterion and limiting value of complex modulus be applied to dynamic equi-biaxial cyclic loading of swollen amorphous rubbers?

In consequence a programme of equi-biaxial dynamic testing ensued. Johannknecht *et al* [72] had already demonstrated that controlled bubble inflation was a feasible method of analysing equi-biaxial stress-strain relations for rubber-like materials. Thereafter, Murphy *et al* [77] created an equi-biaxial dynamic test facility for rubber using the bubble inflation method. Cyclic testing of EPDM samples appeared to show that Abraham's findings for pre-stressing were only applicable for high load ranges, where the material's failure could be anticipated in relatively few cycles.

Hanley [90] developed the cyclic bubble inflation method further and applied it to swollen equi-biaxial disc samples. It was found that the fatigue life results produced in the equi-biaxial tests agreed with those from dynamic uniaxial swelling experiments; that is, the fatigue lives of specimens were reduced in proportion to the amount of swelling. Unsurprisingly, the fatigue life of an EPDM sample under dynamic equi-biaxial loading was greatly reduced in the presence of oil in the rubber network, even for relatively small amounts of swelling. Though only in contact with the oil for an hour at 100 °C, the dynamic properties of complex modulus E* and dynamic stored energy were fundamentally altered from those of untreated EPDM. The changes in these properties and the lower fatigue lives of the swollen specimens were attributed to a number of physical and chemical factors. Physical factors included the presence of larger voids in the network and a lower initial complex modulus due to swelling. Chemical factors included changes in the network structure due to oil swelling, where there may have been a reduction in the number of cross-links resisting the tensile force or where the swelling led to differences in the equilibrium length of individual chains. Also, possibly the reformation of polysulphidic linkages during loading cycles was inhibited in the presence of oil [92].

The relationship between dynamic stored energy and cycles to failure was influenced by the degree of swelling, with the energy at failure reducing as swelling levels increased. It was proposed that a practical approach to predicting realistic fatigue lives in rubber compounds was to use the limiting value of the residual modulus E^*_{res} if the residual modulus for swollen specimens is based on a calculation using the initial conditioned modulus of dry rubber samples at similar stress amplitudes. E^*_{res} values exhibited reasonable correlation with a limiting value of 33%±10% for both the dry and swollen specimens, so by knowing the limiting value of E^*_{res}, (in this case 43% of E^*_{con}), the effect of swelling on fatigue life of

non-strain crystallising rubber components can be determined. Clearly, this approach could have practical significance in the design and maintenance of elastomeric components subjected to fatigue loading conditions. The practical significance of this study was focused on the effect of contamination on the mechanical performance of non-strain crystallizing elastomers subjected to realistic loading conditions. EPDM components are predominantly used in automotive applications, where they provide the advantage of having improved functionality at higher temperatures than SBR or NR. However, some of these advantages are diminished by the material's poor resistance to numerous fluids used in vehicles. Hanley's research illustrated that if a risk of oil contamination is sufficiently high and the automotive design engineer has failed to appreciate the potential detrimental influence of swelling, safety factors may be too small and life expectations for components may be unrealistically high.

5.1. The rationale for equi-biaxial bubble inflation fatigue testing of rubber

The broad outcome of the research described in this chapter is that dynamic equi-biaxial bubble inflation provides rubber technologists with a robust and adaptable method of determining fatigue resilience in elastomeric materials. Physical testing is possible under a wide range of amplitude controls, pre-stressing is easily incorporated into testing, results scatter is reduced and the study of numerous other viscoelastic phenomena in rubber is simply achieved. The test facility is under continuous development to provide viscoelastic material data for loading regimes experienced in 'real world' applications. Most recently, the equi-biaxial bubble inflation system has undergone design changes to deliver dynamic characterisation of the physical properties of magnetorheological elastomers (MREs) [93].

Author details

Steve Jerrams and Niall Murphy
Centre for Elastomer Research (CER), Dublin Institute of Technology, Ireland

John Hanley
FDT Consulting Engineers and Project Managers, Dublin, Ireland

Acknowledgement

The authors wish to express their gratitude to all of the researchers who have participated in the various elastomer fatigue programmes described in this chapter, but in particular to Thomas Alshuth, Raphaël Johannknecht, Georg Clauss, Frank Abraham, Stefan Robin and John McNamara. They also place on record their sincere thanks to the Deutsches Institut für Kautschuktechnologie e.V for an enduring research partnership and to Enterprise Ireland who supported the design and development of the Dynamet equi-biaxial dynamic bubble inflation system under its 'Proof of Concept' programme.

6. References

[1] Mars W, Fatemi A (2004) Factors that Affect the Fatigue Life of Rubber: A literature Survey, Rubber Chemistry and Technology, Vol 77, No 3, 391-312.
[2] Lake G (1995) Rubber Chemistry and Technology. 68, 435.
[3] Thomas A (1994) Rubber Chemistry and Technology. 67, G50.
[4] Ellul M, (1991) 'Mechanical Fatigue', Engineering with Rubber – How to design rubber components, Editor Gent A, Hanser Verlag, Berlin, Germany, Chapter 6, 129.
[5] Young D (1991) Fatigue and fracture of elastomeric materials, Rubber World.
[6] Bauman T (2008) Selecting Strain Amplitude, Fatigue Stress and Strain of Rubber Components: Guide for Design Engineers, Hanser, ISBN: 978-3-446-41681-9, 8.2.2, 118.
[7] Mars W, Fatemi A (2004) Factors that Affect the Fatigue Life of Rubber: A literature Survey, Rubber Chemistry and Technology, Vol 77, No 3, 398.
[8] Kadir A, Thomas A (1981) Tear behavior of rubbers over a wide range of rates. Rubber Chemistry and Technology 54:15–23.
[9] Mazich K, Morman K, Oblinger F, Pan T, Killgoar P, (1989) The effect of specimen thickness on the tearing energy of a gum vulcanizate, Rubber Chemistry and Technology, 62:850–62.
[10] Lindley P (1974) Non-relaxing crack growth and fatigue in a non-crystallizing rubber, Rubber Chemistry and Technology 47:1253–1264.
[11] Beatty J (1964) Fatigue of rubber, Rubber Chemistry and Technology, 37, 1341–1364.
[12] Hardy D, Moneypenny H, Holderied M, Harris J, Campion R, Morgan G (1999) Influence of low surface area carbon blacks on air permeation and fracture mechanical behaviour of tyre innerliner compounds, Rubber Chem 99, Antwerp, Belgium.
[13] Gent A, Hirakawa H (1968) Rubber Chemistry and Technology, Vol. 41, 1294-1299.
[14] Gent A, Hirakawa H (1968) Journal of Polymer Science A-2 6, 1481.
[15] Kim S, Lee S (1994) Rubber Chemistry and Technology, Vol. 67, 649.
[16] Gent A, Hindi M (1990) Effect of oxygen on the tear strength of elastomers. Rubber Chemistry and Technology Vol 63:123–34.
[17] Zhao J, Ghebremeskel G (2000) Rubber Plast. News, 27, 14.
[18] Busfield J, Jha V, Liang H, Papadopoulos I, Thomas A (2005) Prediction of fatigue crack growth using finite element analysis techniques applied to three dimensional elastomeric components, Plastics , Rubbers, Composites, Vol. 34 349-356.
[19] Sakulkaew K, Thomas A, Busfield J (2012) A new approach to categorize the onset of tearing in rubber, Constitutive Models for Rubber VII, Editors Jerrams S and Murphy N, CRC Press, ISBN 978-0-415-68389-0, 185-189.
[20] Marco Y, Le Saux V, Calloch S, Charrier, P (2012) Heat-build up and micro-tomography used to describe the fatigue mechanisms and to evaluate the fatigue lifetime of elastomers, Constitutive Models for Rubber VII, Editors Jerrams S and Murphy N, CRC Press, ISBN 978-0-415-68389-0, 347-352.
[21] Le Chenadec Y, Raoult I, Stolz C, Nguyen-Tajan M, (2009) Cyclic approximation of the heat equation in finite strains for the heat build-up problem of rubber, Journal of Mechanics of Materials and Structures 4 (2) 309-318.

[22] Le Saux V, Marco Y, Calloch S, Doudard C, Charrier P (2010) Fast evaluation of the fatigue lifetime of rubber-like materials based on a heat build-up protocol and microtomography measurements, International Journal of Fatigue 32, 1582-1590.
[23] Beurrot S, Huneau B, Verron E, Rublon P, Thiaudière D, Mocuta C, Zozulya A (2012) In-situ synchtron X-ray diffraction study of strain-induced crystallisation of natural rubber during fatigue tests, Constitutive Models for Rubber VII, Editors Jerrams S and Murphy N, CRC Press, ISBN 978-0-415-68389-0, 353-358.
[24] Le Cam J-B, Toussaint E, (2012) The mechanism of fatigue crack growth in rubbers under severe loading: The effect of stress induced crystallisation, Constitutive Models for Rubber VII, Editors Jerrams S and Murphy N, CRC Press, ISBN 978-0-415-68389-0, 69-75.
[25] Hainsworth S (2007) An environmental scanning electron microscopy investigation of fatigue crack initiation and propagation in elastomers, Polymer Testing 26, 60-70.
[26] Le Cam J-B, Toussaint E (2012) The mechanism of fatigue crack growth in rubbers under severe loading: The effect of stress induced crystallization, Constitutive Models for Rubber VII, Editors Jerrams S and Murphy N, CRC Press, ISBN 978-0-415-68389-0, 69-75.
[27] Le Cam J-B, Toussaint E (2008) Volume variation in stretched natural rubber: competition between cavitation and stress induced crystallisation, Macromolecules 41, 7579- 7583.
[28] Alshuth T, McNamara J, Jerrams S (2007) Improving the Prediction of Stress Softening in Rubber Components, Kautschuk, Gummi, Kunststoffe (KGK) Iss 12.
[29] Busfield J, Thomas a, Ngah M (1999) Application of fracture mechanics for the fatigue life prediction of carbon black filled elastomers, Constitutive Models for Rubber, Editors Dorfman A, Muhr A, 249-256, Balkema, ISBN 9058091139.
[30] Thomas A (1994) The development of fracture mechanics for elastomers, Rubber Chemistry and Technology, Charles Goodyear Medal Address.
[31] Alshuth T, Abraham F, Jerrams S (2002) Parameter Dependence and Prediction of Fatigue Properties of Elastomer Products. Rubber Chemistry and Technology, 75, 365.
[32] Griffith A, Phil. Trans. Royal Society, London,Ser. A 221 11929 163.
[33] Rivlin R, Thomas A (1965) Rupture of Rubber, 1, Characteristic Energy for Tearing. Journal of Polymer Science. Vol 10, No. 3, 291.
[34] Ellul M, (1991) Engineering with Rubber – how to design rubber components, Ch. 6 Mechanical Fatigue, Editor A.N Gent, Hanser Verlag, Berlin, Germany, 129.
[35] Lake G, Lindley P (1965) The Mechanical Fatigue Limit for Rubber', Journal of Applied Polymer Science. Vol 9, 1233.
[36] Seldén R (1995) Fracture Mechanics Analysis of Fatigue of Rubber – A Review, Progress in Rubber and Plastics Technology. 11, 56 – 83.
[37] Wöhler A (1870) Über Festigkeitsversuche mit Eisen und Stahl, Zeitschrift Bauwesen 20, Spalten 73-106.
[38] Gent A (1994) Strength of Elastomers, Science and Technology of Rubber, Editors Mark J, Erman B, Eirich F, 2nd ed., Academic Press, Ch No. 10, 471 - 512.

[39] Lake G, (1972) Mechanical Fatigue of Rubber, Rubber Chemistry and Technology, 45, 309.
[40] Lindley P, (1974) Non-Relaxing Crack Growth and Fatigue in a Non-Crystallizing Rubber, Rubber Chemistry and Technology, 47, 1253.
[41] Cadwell S, Merrill R, Sloman C, Yost F (1940) Ind. Eng. Chem., Anal. Ed., 12, 19.
[42] Fielding J (1943) Ind. Eng. Chem. 35, 1259.
[43] Berry J (1972) Fracture of Non-Metals and Composites, Fracture: An Advanced Treatise, Vol 7, Ch. 2, Editor Liebowitz H, Academic Press, New York.
[44] Jerrams S, Tabakovic A (2001) The Influence of Mean Stress on the Fatigue Properties of Natural Rubber, IRC 2001, Birmingham, UK, 327.
[45] Lee D, Donovan J (1987) Microstructural Changes in the Crack Tip Region of Carbon Black Filled Natural Rubber, Rubber Chemistry and Technology, 60 910.
[46] Lake G, Samura A, Teo S, Vaja J (1991) Polymer, 32, (16), (1991) 2963.
[47] Abraham F (2002) The Influence of Minimum Stress on the Fatigue Properties of Non Strain-Crystallising Elastomers, PhD thesis, Coventry University, Coventry, UK.
[48] Seldén R (1995) Fracture mechanics analysis of fatigue of rubber – a review, Progress in Rubber and Plastics Technology, Vol 11, 1, The Institute of Materials/RAPRA.
[49] Jerrams S, Hanley J, Murphy N, Ali H (2008) Equi-biaxial Fatigue of Elastomers – The Effect of Oil Swelling in Specimen Fatigue Life, Rubber Chemistry and Technology, Vol 81, Issue 4, 638-649.
[50] Abraham F,. Alshuth T, Jerrams S (2005) The effect of minimum stress and stress amplitude on the fatigue life of non strain crystallising elastomers, Journal of Materials and Design, Vol 26, Issue 3, 239-245 (Elsevier).
[51] Alshuth T, Abraham F, Jerrams S (2002) Parameter Dependence and Prediction of Fatigue Properties of Elastomer Products, Rubber Chemistry and Technology, Vol 75, Issue 4, 365.
[52] Abraham F, Alshuth T, Jerrams S (2001) Dependence on mean stress and stress amplitude of fatigue life of EPDM elastomers, Institute of Materials, Vol 30 No. 9 421-425, ISSN 1465-8011.
[53] Mullins L, (1969) Rubber Chemistry and Technology, 42, 339.
[54] Clauss G (1999) Das Hysteresis-Messverfahren zur dynamischen Prüfung von Kunststoffen - ein Verfahren zur Lebensdauervorhersage auch für Elastomer-Bauteile, Lebensdauer und Ermüdung von Elastomeren, DIK Fortbildungsseminar, Hannover, Germany.
[55] James A, Green A, Simpson G (1975) Strain energy functions of rubber, 1: Characterisation of gum vulcanisates, Journal of Applied Polymer Science, 19.
[56] Alshuth T, Abraham F, Jerrams S (2002) Parameter Dependence and Prediction of Fatigue Properties of Elastomer Products. Rubber Chemistry and Technology, 75, 365.
[57] Abraham F (2002) The Influence of Minimum Stress on the Fatigue Properties of Non Strain-Crystallising Elastomers, PhD thesis, Coventry University, Coventry, United Kingdom, 52-57.

[58] Abraham F, Alshuth T, Clauss G (2005) Testing and simulation of the influence of glass spheres on fatigue life and dynamic crack propagation of elastomer. Constitutive Models for Rubber IV, Editors Austrell P, Kari, L, Balkema, ISBN: 0415383463.
[59] Mc Namara J (2011) PhD thesis, Dublin Institute of Technology, Ireland, Novel approaches to the analysis of localised stress concentrations in deformed elastomers, 126-130.
[60] Mc Namara J, Jerrams S, Alshuth T, Robin S (2010) New insights into the distribution and size of flaws in rubber compounds produced by commercial processes, Materials Ireland Conference.
[61] Kingston J, Muhr A (2012) Determination of effective flaw size for fatigue life prediction, Constitutive models for Rubber VII, Editors Jerrams S and Murphy N, ISBN 978-0-415-68389-0, 337-342.
[62] Flint, C, Naunton W (1937) Physical Testing of Latex Films, Transactions of The Institution of the Rubber Industry, Volume 12, P.367-406.
[63] Treloar L (1944) Strains in an Inflated Rubber Sheet, and the Mechanism of Bursting, Rubber Chemistry and Technology, 17, 957-967.
[64] Adkins J, Rivlin R (1952) Large elastic deformations of isotropic materials. XI The deformation of thin shells, F.R.S., Vol. 244, A. 888.
[65] Bhate P, Kardos J (1984) A Novel Technique for the Determination of High Frequency Equi-biaxial Stress-Deformation Behaviour of Viscoelastic Elastomers, Polymer Engineering and Science, Vol. 24, No. 11.
[66] Kong D, White J (1986) Inflation Characteristics of Unvulcanised Gum and Compounded Rubber Sheets, Rubber Chemistry and Technology, 59, 315-327.
[67] Song W, Mirza F, Vlachopoulos J (1991) Finite element analysis of inflation of an axisymmetric sheet of finite thickness, The Society of Rheology, Inc.
[68] Khayat R, Derdouri A (1995) Stretch and Inflation of Hyperelastic Membrane as Applied to Blow Molding, Polymer Engineering and Science, Vol. 35, No. 23.
[69] Mott P, Roland C, Hassan S (2003) Strains in an Inflated Rubber Sheet, Rubber Chemistry and Technology, 76, 326-333.
[70] Johannknecht R (1999) The Physical Testing and Modelling of Hyperelastic Materials for Finite Element Analysis, PhD Thesis, (Coventry University in collaboration with Robert Bosch GmbH).
[71] Johannknecht R, Jerrams S, (1999) The need for equi-biaxial testing to determine elastomeric material properties, Constitutive Models for Rubber, Editors Dorfman A, Muhr A, 73-76, Balkema, ISBN 9058091139.
[72] Johannknecht R, Jerrams S, Clauss G (2002) Determination of non-linear, large equal biaxial stresses and strains in thin elastomeric sheets by bubble inflation, Proceedings of the Institute of Mechanical Engineers, Vol 216 Part L, No L4, 233-243, (ISSN 1464-4207) Journal of Materials, Design and Applications.
[73] Johannknecht R, Clauss G, Jerrams S (1997) The Uncertainty of Implemented Curve Fitting Procedures in Finite Element Software, Finite Element Analysis of Elastomers. IMechE Seminar, Finite Element Analysis of Elastomers, 141-151.

[74] Murphy N (2010) Providing Stress Controlled Equi-Biaxial Fatigue Test Data for Elastomers using the Bubble Inflation Method, PhD thesis, Dublin Institute of Technology.
[75] Bhate P, Kardos J (1984) A Novel Technique for the Determination of High Frequency Equi-biaxial Stress-Deformation Behaviour of Viscoelastic Elastomers, Polymer Engineering and Science, Vol. 24, No. 11.
[76] Hallett, J (1997) Multi-axial Strength and Fatigue of Rubber Compounds, PhD Dissertation, Loughborough University, England.
[77] Murphy N, Jerrams S,Hanley J, McCartin J, Lanigan B, McLoughlin S, Clauss G, Johannknecht R (2005) Determining Multiaxial Fatigue in Elastomers using Bubble Inflation, Constitutive Models for Rubber IV', Editors Rustrell P, Kari L, 65-70, Balkema, ISBN 0 415 38346 3.
[78] Murphy N, Hanley J, Jerrams S (2009) The Effect of Pre-Stressing on the Equi-Biaxial Fatigue Life of EPDM, Constitutive Models for Rubber VI. Editors Heinrich G, Kaliske M, Lion A, Reese S, 269-273, CRC Press, ISBN: 978-3-00-025427-7
[79] Murphy N, Hanley J, Ali H, Jerrams S (2007) The Effect of Specimen Geometry on the Multi-axial Deformation of Elastomers, Constitutive Models for Rubber V, Editors Boukamel A, Laiarinandrasana L, Meo S and Verron E, 61-65, Taylor and Francis, ISBN 0415454425.
[80] McLoughlin S, Murphy N, Hanley J, Lanigan B, Markham C (2005) Measuring biaxial strain in rubber using stereo vision, Proceedings of the Irish Machine Vision and Image Processing Conference, IMVIP2005, Belfast.
[81] Murphy N, Jerrams S, Spratt C, Ronan S (2003) A test rig to provide multi-axial fatigue data in elastomers, Matrib, Velaluka, Croatia.
[82] Murphy N, Jerrams S, Spratt C, Ronan S, Johannknecht R (2003) Method for determining equi-biaxial fatigue in elastomers, Constitutive Models for Rubber III, Editors Busfield J, Muhr A, 21-26, Balkema, ISBN 9058095665.
[83] Cho K, Wook J, Daeho L, Hyunaee C, Young-Wook C, (2000) Polymer. 41, 179.
[84] Gul V, Fedyukin D, Dogadkin B, (1959) Rubber Chemistry and Technology 32, 454.
[85] Dogadkin A, Gul V, (1951) Rubber Chemistry and Technology 24, 344.
[86] Neogi C, Bhattacharya A, Bhowmick A, (1990) Rubber Chemistry and Technology 63, 651.
[87] Beerbower A, Pattison D, Staffin G, (1964) Rubber Chemistry and Technology. 37, 246.
[88] Abhimanyu P, Coolbaugh T, (2005) Rubber Chemistry and Technology 78, 516.
[89] Flory P, Rehner J, (1943) Statistical Mechanics of Cross-Linked Polymer Networks II. Swelling, J. Chem. Phys. 11, 521.
[90] Hanley J (2008) Swelling Effects in Dynamic Equi-Biaxial Testing of EPDM Elastomers by the Bubble Inflation Method, PhD thesis, Dublin Institute of Technology (DIT).
[91] ASTM Standard D471-95, (1995) Standard Test Method for Rubber Property-Effect of Liquids, Standard 09.01, 86.
[92] Cho K, Wook J, Daeho L, Hyunaee C, Young-Wook C (2000) Polymer 41, 179.
[93] Chen L, Jerrams S (2011) A rheological model of the dynamic behaviour of magnetorheological elastomers, Journal of Applied Physics 110, 013513.